2012

Hybridization among Arctic white-headed gulls (*Larus* spp.) obscures the genetic legacy of the Pleistocene

Sarah A. Sonsthagen
USGS Alaska Science Center, ssonsthagen@usgs.gov

R. Terry Chesser
USGS Patuxent Wildlife Research Center, terry.chesser@usgs.gov

Douglas A. Bell
California Academy of Sciences, dbell@calacademy.org

Carla J. Dove
Smithsonian Institution, dovec@si.edu

Ecology and Evolution

Open Access

Hybridization among Arctic white-headed gulls (*Larus* spp.) obscures the genetic legacy of the Pleistocene

Sarah A. Sonsthagen[1], R. Terry Chesser[2], Douglas A. Bell[3] & Carla J. Dove[1]

[1]Department of Vertebrate Zoology, Division of Birds, National Museum of Natural History, Smithsonian Institution, Washington, DC 20013
[2]USGS Patuxent Wildlife Research Center, National Museum of Natural History, Smithsonian Institution, Washington, DC 20560
[3]Department of Ornithology and Mammology, California Academy of Sciences, 55 Music Concourse Drive, Golden Gate Park, San Francisco, California 94118

Keywords
Genetic structure, hybridization, *Larus*, Pleistocene glacial refugia, white-headed gulls.

Correspondence
Sarah Sonsthagen, Alaska Science Center, US Geological Survey, Anchorage, AK 99508.
Tel: 907-786-7054; Fax: 907-786-7020;
E-mail: ssonsthagen@usgs.gov

Received: 30 August 2011; Revised: 10 February 2012; Accepted: 13 February 2012

Ecology and Evolution **2012; 2(6): 1278–1295**

doi: 10.1002/ece3.240

Abstract

We studied the influence of glacial oscillations on the genetic structure of seven species of white-headed gull that breed at high latitudes (*Larus argentatus*, *L. canus*, *L. glaucescens*, *L. glaucoides*, *L. hyperboreus*, *L. schistisagus*, and *L. thayeri*). We evaluated localities hypothesized as ice-free areas or glacial refugia in other Arctic vertebrates using molecular data from 11 microsatellite loci, mitochondrial DNA (mtDNA) control region, and six nuclear introns for 32 populations across the Holarctic. Moderate levels of genetic structure were observed for microsatellites ($F_{ST} = 0.129$), introns ($\Phi_{ST} = 0.185$), and mtDNA control region ($\Phi_{ST} = 0.461$), with among-group variation maximized when populations were grouped based on subspecific classification. Two haplotype and at least two allele groups were observed across all loci. However, no haplotype/allele group was composed solely of individuals of a single species, a pattern consistent with recent divergence. Furthermore, northernmost populations were not well differentiated and among-group variation was maximized when *L. argentatus* and *L. hyberboreus* populations were grouped by locality rather than species, indicating recent hybridization. Four populations are located in putative Pleistocene glacial refugia and had larger τ estimates than the other 28 populations. However, we were unable to substantiate these putative refugia using coalescent theory, as all populations had genetic signatures of stability based on mtDNA. The extent of haplotype and allele sharing among Arctic white-headed gull species is noteworthy. Studies of other Arctic taxa have generally revealed species-specific clusters as well as genetic structure within species, usually correlated with geography. Aspects of white-headed gull behavioral biology, such as colonization ability and propensity to hybridize, as well as their recent evolutionary history, have likely played a large role in the limited genetic structure observed.

Population and species divergence in Arctic breeding species often reflect the climatic oscillations of the Pleistocene (Hewitt 2004). Glacial activity had profound effects on the distribution of Arctic taxa through these major climatic shifts. During glacial maxima, ice sheets subdivided ancestral populations into temperate or high-latitude ice-free areas, often resulting in the formation of phenotypically similar species with shallow genetic differentiation (Schmitt 2007). Warming during interglacial periods allowed species to expand their distributions into newly available habitat, resulting in clinal variation in genetic diversity (Hewitt 2004). This pattern of expansion and contraction of species distributions occurred many times in the Pleistocene; more than 20 glacial cycles have been recorded (Williams et al. 1998). Following the glacial maxima, many species that were isolated in southern and northern refugia expanded, came into secondary contact, and hybridized to varying extents (Hewitt 2001). This likely resulted in cycles of isolation and hybridization throughout

the Pleistocene. Concordance of secondary contact zones (suture zones) has been observed across several Arctic species, which suggests a commonality in the location and persistence of glacial refugia during the last glacial maximum (Hewitt 2000).

Over the past decade, molecular markers have aided in the identification of cryptic glacial refugia and substantiated previously hypothesized refugia (Waltari and Cook 2005; Schafer et al. 2010; Sonsthagen et al. 2011). Previously, identification of the location of Pleistocene glacial refugia required knowledge of species distributions prior to glaciations or were inferred from paleoecological data. However, population contractions and expansions as a result of glacial cycling left predictable genetic signatures (Avise 2000). Populations arising via postglacial colonization of a region through successive founder events are expected to show reduced genetic diversity relative to populations residing in nonglaciated areas and to exhibit a genetic signature of population expansion from low-diversity founder populations (Galbreath and Cook 2004). However, current or past hybridization among closely related taxa may make it difficult to assess genetic relationships among Arctic populations. Introgression would likely have maintained or increased genetic diversity when a recently deglaciated area was colonized, and, therefore, would not be expected to produce a genetic signature of population expansion.

White-headed gulls (*Larus* spp.) are a geographically widespread clade of 18 species (Liebers et al. 2004; Olsen and Larsson 2004; Pons et al. 2005). Included in this clade is a subclade of 13 very closely related species of large white-headed gulls (Pons et al. 2005), which present particularly vexing problems to biologists. Some species within the white-headed gull complex have a circumpolar distribution (*L. argentatus*, *L. canus*, and *L. hyperboreus*; Fig. 1), while others are restricted to more circumscribed areas at high latitude (*L. glaucoides, L. schistisagus,* and *L. thayeri*; Fig. 1; Olsen and Larsson 2004). Previous assessments of relationships among white-headed gull populations revealed low to moderate genetic structure based on mitochondrial DNA (mtDNA), microsatellite, and amplified fragment length polymorphism (AFLP) loci (Liebers et al. 2001; Liebers and Helbig 2002; Crochet et al. 2003; Liebers et al. 2004; Pons et al. 2005; Gay et al. 2007; Vigfúsdóttir et al. 2008; Sternkopf et al. 2010). However, these studies focused largely on populations in Europe where climatic oscillations of the late Quaternary were significantly different than those in North America (Hewitt 1996), notably in the extensive glacial advances in North America (Velichko et al. 1997) and the likely absence of long-term high-latitude glacial refugia in Europe (Schmitt 2007). The presence of several white-headed gull species restricted to northern latitudes, coupled with the relatively low genetic differentiation observed among taxa, suggests that glacial oscillations associated with the late Pleistocene may have played a large role in the diversification of this group.

We studied the influence of glacial oscillations on the genetic structure of seven species of white-headed gull that breed at high latitudes (*L. argentatus, L. canus, L. glaucescens*, *L. glaucoides*, *L. hyperboreus*, *L. schistisagus*, and *L. thayeri*) using microsatellite genotypes from 11 autosomal loci, intron sequences from six autosomal nuclear genes, and mtDNA sequences from the control region. We evaluated Holarctic localities that have been hypothesized as ice-free areas or glacial refugia in other Arctic vertebrates, including the southern edge of the Bering Land Bridge, northern Beringia, Haida Gwaii, Newfoundland Bank, Spitsbergen Bank, and northwest Norway. Specifically, we employed traditional frequency-based and coalescent-based analyses to test if populations residing at high latitudes have the genetic signature of refugia. Populations formed through postglacial colonization are characterized by lower levels of nucleotide and haplotype diversity (Avise 2000), later times of expansion relative to other sampled populations, and genetic signatures of population growth based on the coalescent (Lessa et al. 2004). Inclusion of multiple taxa that occupy the Arctic allow us to examine whether geographically concordant contact regions suggestive of secondary contact are observed among populations expanding out of different Pleistocene refugia (i.e., suture zones) (Avise 2000).

Methods

Sampling and DNA extraction

Tissue samples of breeding-season adults, representing seven species and 32 populations of white-headed gulls, were collected or obtained through tissue loans (Fig. 1; Appendix S1): *L. argentatus argentatus* (Norway), *L. a. argenteus* (France, Iceland, and United Kingdom), *L. a. smithsonianus* (Canada and United States), *L. canus brachyrhynchus* (Canada and United States), *L. c. canus* (Sweden and United Kingdom), *L. c. kamtschatschensis* (Russia), *L. glaucescens* (Canada and United States), *L. glaucoides kumlieni* (Canada), *L. hyperboreus barrovianus* (United States), *L. h. hyperboreus* (Canada, Greenland, Iceland, and Norway), *L. h. pallidissimus* (Russia), *L. schistisagus* (Russia and United States), and *L. thayeri* (Canada and United States). Because of the limited number of breeding individuals of *L. thayeri* in tissue collections, nonbreeding adults of this species were included in this study. Care was taken to ensure that plumage characteristics were consistent with pure species, given the tendency for hybridization in this group (Pierotti 1987; Olsen and Larsson 2004 and citations therein). Species classifications follow the American Ornithologists' Union Checklist of North American Birds (Banks et al. 2008); individuals were diagnosed to subspecies based on morphological characteristics

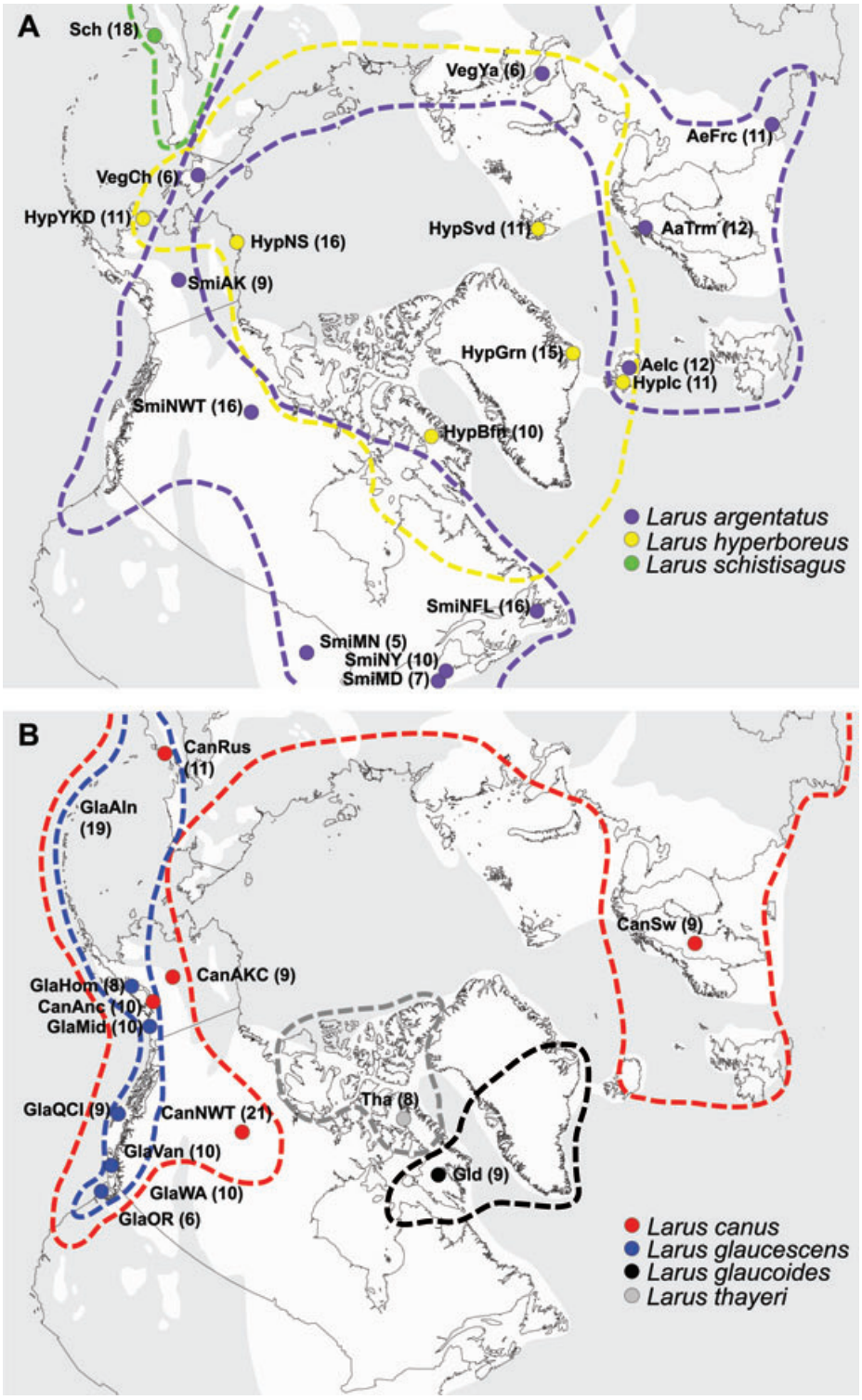

Figure 1. Seven Arctic gull species distributions and localities of 32 populations used in this study: (A) *Larus argentatus* (Aa, Ae, Smi, and Veg), *L. hyperboreus* (Hyp), *L. schistisagus* (Sch), and (B) *L. canus* (Can), *L. glaucescens* (Gla), *L. glaucoides* (Gld), and *L. thayeri* (Tha). Extent of the most recent glacial ice sheets is illustrated in white, and unglaciated regions are illustrated in gray (Hewitt 2004). Sample sizes are in parentheses. See Appendix S1 for physical descriptions of the localities.

(Olsen and Larsson 2004). Total genomic DNA was extracted from each sample using an AutoGen animal tissue extraction kit (AutoGen, Holliston, Maine). Genomic DNA concentrations were quantified using spectrophotometry and diluted to 50 ng μL^{-1} working solutions.

Microsatellite genotyping

Twenty-four individuals were screened at 30 microsatellite loci known to be variable for gull species (*Laridae*). Of these, 11 polymorphic loci containing dinucleotide repeat motifs were selected for further analyses of all tissue samples: Hg16, Hg18, Hg25 (Crochet et al. 2003), K16 (Tirard et al. 2002), LarZAP12, LarZAP19, LarSNX24, LarZAP26 (Gregory and Quinn 2006), Rbg13, Rbg18, and Rbg29 (Given et al. 2002). Polymerase chain reaction (PCR) amplifications followed Sonsthagen et al. (2007) with two modifications. The forward primer was end-labeled with one of two fluorescent phosphoramidite dyes (FAM or HEX). Fluorescently labeled PCR products were electrophoresed on an automated DNA sequencer (ABI 3130XL; Applied Biosystems, Foster City, CA) and sized using GENEMAPPER® version 4.0 (Applied Biosystems) with a universal ROX-labeled size standard (DeWoody et al. 2004). Ten percent of the samples were amplified and sized in duplicate for quality control purposes.

MtDNA and nuclear intron sequencing

We followed Liebers et al. (2001) and amplified a 2500 base pair (bp) fragment of the mtDNA genome to avoid amplifying nuclear pseudogenes observed in this group. From this, we directly sequenced 430 bp of domain I of the control region. Twenty nuclear autosomal introns were screened for variability and six selected for further analysis: α–enolase intron 8, ghrelin (*ghrel*) intron 3, ornithine carboxylase (*od*) intron 7, clathrin heavy-chain (*chc*) intron 5, myelin proteolipid protein (*mpp*) intron 4, and glyceraldehyde-3-phosphate dehydrogenase (*gapdh*) intron 11. *Ghrel* had two insert/deletions. To obtain sequence information from the entire fragment for individuals that are heterozygous for both insert/deletions, two internal sequencing primers were developed. See Appendix S2 for primer information. PCR amplifications, cycle sequencing, and postsequencing protocols followed Sonsthagen et al. (2007). ExoSAP-IT® (USB Corporation, Cleveland, OH) was used to remove excess primers and dNTPs in PCR products. Sequences are accessioned in GenBank (JQ708216–JQ710335).

Estimation of genetic diversity

Allelic phases of nuclear introns were inferred from diploid sequence data using PHASE 2.0 (Stephens et al. 2001). PHASE uses a Bayesian approach to reconstruct haplotypes from population genotypic data and allows for recombination and the decay of linkage disequilibrium with distance. The accuracy of haplotypes reconstructed by PHASE has been validated and shown to be greater than that of cloning with large datasets (Harrigan et al. 2008). The PHASE analysis (1000 iterations with a 1000 iteration burn-in period) was repeated three times and was consistent across runs. MtDNA and nuclear intron sequences were analyzed in NETWORK 4.5.0.0 (Fluxus Technology Ltd. 2008) using the median joining method (Bandelt et al. 1995), to illustrate possible reticulations in the gene trees because of homoplasy or recombination.

We calculated allelic frequencies, inbreeding coefficient (F_{IS}), and expected and observed heterozygosities for each microsatellite locus, mtDNA, and the six nuclear introns in FSTAT 2.9.3 (Goudet 1995). Hardy–Weinberg equilibrium (HWE) and linkage disequilibrium were tested in FSTAT 2.9.3 for microsatellite and nuclear intron loci, adjusting for multiple comparisons using Bonferroni corrections ($\alpha = 0.05$). We verified the selective neutrality for mtDNA control region sequence data using Tajima's *D* (Tajima 1989), implemented in ARLEQUIN 3.11 (Schneider et al. 2000).

Detecting spatial genetic structure

Levels of population structure among sampled sites were assessed with pairwise F_{ST}, R_{ST}, Φ_{ST}, overall *F*-statistics, and *R*-statistics calculated in ARLEQUIN, adjusting for multiple comparisons using Bonferroni correction ($\alpha = 0.05$). We used Hedrick's (2005) method, implemented in RecodeData version 1.0 (Meirmans 2006) to calculate the maximum value of F_{ST} obtainable for our suite of microsatellite loci. Interallelic and interhaplotypic sequence divergences were used to calculate pairwise Φ_{ST} (Excoffier et al. 1992), and nuclear intron alleles were paired by individual. MODELTEST 3.06 (Posada and Crandall 1998) was used to determine the minimum parameter nucleotide substitution model that best fit the nuclear intron and mtDNA sequence data under Akaike's information criterion (Appendix S2; Akaike 1974).

Genotypic nuclear data (microsatellite and intron) were analyzed in STRUCTURE 2.2.3 (Pritchard et al. 2000) to detect the occurrence of population structure without a priori knowledge of putative populations. A series of analyses were performed (1) among large white-headed gull individuals (excludes *L. canus* individuals; Pons et al. 2005), and (2) within species represented by multiple populations. Data were analyzed using an admixture model assuming correlated frequencies to probabilistically assign individuals to putative populations (parameters: burn-in 10,000 iterations; 500,000 Markov chain Monte Carlo iterations) with the possible populations (*K*) ranging from 1 to 15. Analyses were repeated five times and were consistent across runs. We used the method

of Evanno et al. (2005) to determine the most likely number of clusters.

Hierarchical analyses of molecular variance (AMOVA) were conducted in ARLEQUIN to test for significance of geographic and taxonomic (subspecies and species) partitioning of a priori hypothesized genetic units using microsatellite, nuclear intron, and mtDNA loci. Populations were grouped to test (1) specific designations, (2) subspecific designations, (3) geographic proximity irrespective of species status, and (4) geographic proximity and species status. We assumed that groupings that maximized the among-group variance (Φ_{CT}) and were significantly different from random distributions constituted the most probable subdivision (Sonsthagen et al. 2011). *L. glaucoides*, *L. schistisagus*, and *L. thayeri* were not included in AMOVA comparisons because these species were represented by a single population.

Estimation of population demography

Evidence for historical fluctuations in population size was evaluated for 11 microsatellite loci using BOTTLENECK 1.2.02 (Cornuet and Luikart 1996) and for sequence data using LAMARC 2.1.2b (Kuhner 2006; Kuhner and Smith 2007). Fluctuations in population size inferred from microsatellite data were assessed using a Wilcoxon sign-rank test in BOTTLENECK. The probability distribution was established using 1000 permutations under two models: stepwise mutation model (SMM) and two-phase model of mutation (TPM; parameters: 79% SMM, variance 9; Rousset 1996). Heterozygote deficiency relative to the number of alleles indicates recent population growth, whereas heterozygote excess indicates a recent population bottleneck (Cornuet and Luikart 1996). It is important to note that BOTTLENECK compares heterozygote deficiency and excess relative to genetic diversity, not to HWE expectation (Cornuet and Luikart 1996). LAMARC was run using Bayesian search parameters: 10 short chains (1000 trees used out of 20,000 sampled) and three long chains (10,000 trees used out of 2,000,000 sampled). Data were analyzed three times and parameters converged across runs. Finally, mismatch distributions of mtDNA haplotype data were calculated in ARLEQUIN to gain further insight into historical population demography (Rogers and Harpending 1992).

Results

Genetic diversity

Multilocus microsatellite genotypes were collected from 343 individuals representing seven species. The number of alleles per locus ranged from 4 to 18. Allelic richness ranged from 1.62 to 2.86 with a mean of 2.62 across all populations (Table 1). Observed heterozygosities ranged from 22.7% to 70.7%; the mean across all populations was 52.0% (Table 1). In general, *L. hyperboreus* and populations of *L. argentatus* from Europe had lower levels of heterozygosity than did other species. Two populations (AeFrc and CanNWT) exhibited heterozygote deficiency and did not conform to HWE (Table 1). The population of *L. canus* from the Northwest Territories (CanNWT) was in linkage disequilibrium at nine loci pairs (Lar24xK16, Lar24xHg18, Lar12xLar19, Lar12xK16, Lar12xHg18, Lar12xRbg29, Lar26xHg18, Lar19xHg18, K16xHg18), but the overall comparison was not significant. The remaining populations and loci were in linkage equilibrium and HWE and all loci were retained for subsequent analyses. The inbreeding coefficient (F_{IS}) ranged from –0.098 to 0.286 across populations; mean value was 0.112. The inbreeding coefficient for CanNWT was significantly larger than expected ($\alpha > 0.05$) (Table 1).

Nuclear introns were 323–665 bp in length and contained 15–46 variable sites (Appendix S2). PHASE reconstructed 24–117 alleles for the individual introns (Fig. 2A–F; Appendix S2). Probabilities of reconstructed haplotypes ranged primarily from 0.80 to 1.00, although a minority of individuals had probabilities ranging from 0.50% to 0.78 (5% of individuals for *chc*, 2% for *enolase*, 12% for *gapdh*, 2% for *ghrel*, 17% for *mpp*, and 2% for *od7*). We attribute the lower probabilities of reconstructed haplotypes for *gapdh* and *mpp* to the high occurrence of autapomorphies (single novel polymorphisms occurring on one allele in one individual) in these loci; 30% and 18% of individuals had novel polymorphisms for *gapdh* and *mpp*, respectively. Private alleles were observed for most species at most loci; however, private alleles were only observed in two (*enolase* and *gapdh*) or three (*chc*, *enolase*, and *gapdh*) nuclear introns, respectively, for *L. glaucoides* and *L. thayeri* (Fig. 2A–F). Observed heterozygosities ranged from 47.7% to 77.3%, with a mean of 61.3% across all populations (Table 1). Populations and loci were in linkage equilibrium and HWE. The inbreeding coefficient (F_{IS}) ranged from –0.171 to 0.311, mean value was 0.088. Inbreeding coefficients for CanAnc and CanRus were significantly larger than expected ($\alpha > 0.05$) (Table 1). Haplotype (h) and nucleotide (π) diversity ranged from 0.957 to 1.000 and 0.000 to 0.009, respectively (Table 1).

We assayed a 392 bp fragment of the mtDNA control region characterized by 54 variable sites among 134 unique haplotypes (Appendix S2; Fig. 2G). Number of haplotypes per population ranged from 2 to 14 (mean = 6.48; Table 1). Private haplotypes were observed for all species (Fig. 2G). Haplotype (h) and nucleotide (π) diversity were high for most populations, with values ranging from 0.286 to 1.000 and 0.001 to 0.024, respectively (Table 1). Five populations had significant Tajima's D estimates (CanRus $D = -1.562$, $P = 0.05$; HypIc $D = -1.809$, $P = 0.02$; HypNS $D = -1.867$, $P = 0.02$; HypYKD $D = -1.627$, $P = 0.04$; SmiNWT $D = -1.583$, $P = 0.04$); the remaining estimates were not significant.

Table 1. Expected (H_e) and observed heterozygosities (H_o), haplotype (h) and nucleotide (π) diversity, with standard deviation (SD), allelic richness (AR) or number of haplotypes (H), and sample size (n) estimated from Arctic gull populations based on 11 microsatellite, six nuclear introns, and mtDNA control region loci. Significant estimates ($\alpha = 0.05$) are in bold text.

	Microsatellites				Nuclear introns						mtDNA			
	AR	H_e/H_o	F_{IS}	n	AR	H_e/H_o	F_{IS}	h	π	n	H	h	π	n
Sch	2.58	67.2/59.5	0.118	18	1.65	79.4/76.4	0.039	0.995 (0.009)	0.003 (0.002)	18	10	0.882 (0.063)	0.014 (0.008)	18
Tha	2.55	66.0/63.2	0.045	8	1.75	79.1/74.4	0.064	1.000 (0.009)	0.003 (0.002)	8	6	0.929 (0.084)	0.005 (0.004)	8
Gld	2.31	56.7/47.0	0.181	9	1.75	75.4/65.7	0.137	1.000 (0.019)	0.005 (0.003)	9	5	0.806 (0.120)	0.005 (0.004)	9
VegYa	2.34	59.8/52.1	0.154	6	1.79	61.5/70.3	0.138	1.000 (0.045)	0.009 (0.005)	5	4	0.900 (0.161)	0.007 (0.005)	5
VegCh	2.68	71.4/58.1	0.206	6	1.79	79.0/69.4	−0.171	0.989 (0.031)	0.004 (0.002)	6	5	0.933 (0.122)	0.017 (0.011)	6
SmiAK	2.45	61.0/52.7	0.144	9	1.75	64.1/51.4	0.237	1.000 (0.063)	0.004 (0.003)	4	3	0.833 (0.222)	0.007 (0.006)	4
SmiNWT	2.45	62.1/56.0	0.101	16	1.64	71.4/73.3	−0.028	1.000 (0.004)	0.004 (0.003)	17	11	0.882 (0.072)	0.006 (0.004)	17
SmiMN	2.50	64.4/50.4	0.245	5	1.60	60.2/61.4	−0.029	1.000 (0.044)	0.003 (0.002)	5	3	0.700 (0.218)	0.016 (0.011)	5
SmiMD	2.28	57.0/62.1	−0.098	7	1.62	69.8/69.7	0.004	0.989 (0.031)	0.004 (0.002)	7	5	0.857 (0.137)	0.016 (0.010)	7
SmiNY	2.24	55.4/45.9	0.180	10	1.62	70.7/53.2	0.308	1.000 (0.027)	0.006 (0.003)	7	2	0.286 (0.196)	0.001 (0.001)	7
SmiNFL	2.14	50.9/44.8	0.123	16	1.60	71.4/77.3	−0.089	1.000 (0.009)	0.004 (0.002)	15	5	0.638 (0.129)	0.003 (0.002)	15
AeIc	1.96	44.5/43.2	0.029	12	1.56	56.2/48.6	0.141	0.996 (0.013)	0.003 (0.002)	12	8	0.924 (0.058)	0.018 (0.010)	12
AeFrc	2.21	**52.6/45.8**	0.134	11	1.67	67.1/63.7	0.114	0.957 (0.029)	0.002 (0.001)	11	9	0.946 (0.066)	0.011 (0.007)	11
AaTrm	2.17	53.4/50.0	0.067	10	1.60	59.9/52.7	0.126	1.000 (0.016)	0.003 (0.002)	12	5	0.667 (0.141)	0.015 (0.009)	12
HypYKD	2.35	59.6/58.7	0.015	11	1.58	74.7/65.7	0.131	1.000 (0.014)	0.005 (0.003)	11	8	0.891 (0.092)	0.005 (0.004)	11
HypRus	2.20	53.4/46.9	0.126	16	1.64	63.6/59.8	0.062	0.994 (0.010)	0.004 (0.002)	16	11	0.908 (0.063)	0.009 (0.006)	16
HypBfn	2.09	51.4/53.3	−0.040	10	1.69	62.4/59.3	0.054	1.000 (0.016)	0.003 (0.002)	10	7	0.867 (0.107)	0.008 (0.005)	10
HypGrn	2.17	54.3/47.0	0.140	15	1.68	60.4/55.9	0.079	0.998 (0.009)	0.004 (0.003)	15	7	0.827 (0.082)	0.013 (0.008)	15
HypIc	1.62	30.9/22.7	0.274	11	1.57	60.4/59.1	0.023	1.000 (0.016)	0.003 (0.002)	11	4	0.490 (0.175)	0.005 (0.004)	11
HypSvd	2.09	50.1/45.0	0.107	10	1.55	62.3/55.0	0.122	1.000 (0.014)	0.004 (0.002)	11	5	0.756 (0.130)	0.004 (0.003)	10
GlaAln	2.34	58.0/50.6	0.131	19	1.71	69.3/60.6	0.131	0.999 (0.007)	0.000 (0.000)	19	12	0.935 (0.041)	0.015 (0.008)	18
GlaHom	2.40	60.1/59.8	0.005	8	1.79	67.9/52.1	0.249	1.000 (0.022)	0.004 (0.002)	8	6	0.929 (0.084)	0.010 (0.006)	8
GlaMid	2.40	61.5/55.0	0.113	10	1.62	57.5/56.4	0.019	1.000 (0.016)	0.004 (0.002)	10	10	1.000 (0.045)	0.021 (0.012)	10
GlaQCI	2.34	60.0/56.4	0.065	9	1.66	54.6/50.0	0.088	1.000 (0.019)	0.003 (0.002)	9	9	1.000 (0.052)	0.014 (0.008)	9
GlaVan	2.19	53.5/45.4	0.161	9	1.70	57.5/51.4	0.110	0.995 (0.018)	0.000 (0.000)	10	6	0.889 (0.091)	0.013 (0.008)	9
GlaWA	2.29	57.2/52.8	0.080	10	1.71	64.6/58.3	0.103	1.000 (0.016)	0.006 (0.003)	10	8	0.956 (0.059)	0.019 (0.011)	10

Table 1. Continued

	Microsatellites				Nuclear introns						mtDNA			
	AR	H_e/H_o	F_{IS}	*n*	AR	H_e/H_o	F_{IS}	*h*	π	*n*	H	*h*	π	*n*
GlaOR	2.04	48.0/35.4	0.286	6	1.68	64.4/69.4	−0.087	1.000 (0.034)	0.006 (0.003)	6	4	0.800 (0.172)	0.004 (0.003)	6
CanAKC	2.86	75.6/70.7	0.068	9	1.64	67.5/63.7	0.061	1.000 (0.019)	0.004 (0.002)	9	7	0.964 (0.077)	0.024 (0.014)	8
CanAnc	2.79	73.3/67.7	0.080	10	1.70	66.1/47.7	**0.299**	0.996 (0.015)	0.003 (0.002)	11	10	0.982 (0.046)	0.021 (0.012)	11
CanNWT	2.74	**71.7/60.3**	**0.162**	21	1.60	69.5/64.3	0.077	0.996 (0.006)	0.004 (0.002)	21	14	0.986 (0.022)	0.010 (0.006)	20
CanSw	2.38	58.3/43.9	0.274	5	1.71	74.9/60.7	0.208	1.000 (0.019)	0.004 (0.002)	9	3	0.700 (0.218)	0.004 (0.003)	5
CanRus	2.55	66.2/62.6	0.056	11	1.71	71.0/49.7	**0.311**	1.000 (0.014)	0.004 (0.002)	11	7	0.818 (0.119)	0.014 (0.008)	11
Overall	2.62	58.7/52.0	0.112	343	1.76	75.6/61.3	0.088	–	–	343	6.84	–	–	334

Spatial genetic structure

Analyses among species

Overall estimates of population subdivision were significant across all marker types (microsatellites $F_{ST} = 0.129$, $R_{ST} = 0.211$; nuclear introns $F_{ST} = 0.133$, $\Phi_{ST} = 0.185$; mtDNA $F_{ST} = 0.122$, $\Phi_{ST} = 0.461$; Table 2). RecodeData calculated an upper F_{ST} limit of 0.415 for the microsatellite data. Therefore, the overall F_{ST} of 0.129 accounts for 31.1% of the maximum possible level of genetic structure. Moderate levels of population structure were observed among species at the 11 microsatellite loci and six nuclear loci (Table 2; Appendix S3). Most of the significant interpopulation comparisons among species were observed between *L. glaucescens* populations and all other populations and between *L. canus* populations and all other populations; values were typically higher when a mutation model was applied to the dataset (R_{ST} and Φ_{ST}; Appendix S3). In contrast to the nuclear data, high levels of variance in mtDNA haplotypic frequency were observed between most population pairs. As with the nuclear data, most interpopulation comparisons between *L. canus* and all other species were significant (Appendix S3).

Our STRUCTURE analyses indicated that ΔK was maximized among all large white-headed gull individuals when K equaled 2 ($\Delta K = 327.5$) and 4 ($\Delta K = 16.4$) for the microsatellite and nuclear intron loci, respectively (Fig. 3). Patterns of individual assignment differed slightly between marker types: *L. glaucescens* and *L. schistisagus* individuals were assigned predominantly to one cluster and *L. argentatus* and *L. hyperboreus* individuals to the other cluster based on microsatellite data (Fig. 3A). Gulls representing *L. thayeri*, *L. glaucoides*, and northern populations of *L. argentatus* (AaTrm, SmiAK, SmiMN, VegCh, VegYa) and *L. hyperboreus* (HypYKD) were assigned in approximately equal proportions to both clusters based on microsatellite data (Fig. 3A), a signal consistent with hybridization at the northern locales. Similarly, *L. glaucescens* individuals were predominantly assigned to a single cluster (blue) based on the nuclear intron data, with *L. hyperboreus* and some individuals representing *L. argentatus* (AeFrc, AeIc, AaTrm) predominantly assigned to another cluster (red) (Fig. 3B). The remaining individuals were assigned to the four clusters in approximately equal portions (Fig. 3B).

Partitions in the nuclear and mitochondrial genomes appear to conform to subspecific classifications (Fig. 4). Among-group variation (F_{CT}) based on the microsatellite data was maximized when populations were grouped by subspecies or a combination of subspecies and geographic proximity for F_{ST} and R_{ST} estimates, respectively (Fig. 4). Similarly, among-group variation based on nuclear intron and mtDNA data (F_{ST} and Φ_{ST}) was maximized by subspecies. Because the high level of structure between *L. glaucescens* and *L. canus* populations and all other populations is likely driving variance estimates, we ran additional AMOVAs including only populations of *L. argentatus* and *L. hyperboreus*, the other two species represented by multiple populations, to gain additional insight into the partitioning of genetic variation in these species. Among-group variation, as estimated from microsatellite (F_{ST} and R_{ST}) and nuclear intron frequency data (F_{ST}; Fig. 4), was maximized when *L. argentatus* and *L. hyperboreus* populations were grouped by geographic proximity regardless of specific or subspecific classification. This is suggestive of contemporary hybridization. In contrast, among-group variance estimates calculated from the mtDNA (F_{ST} and Φ_{ST}) and nuclear intron (Φ_{ST}) sequence data were maximized when populations were grouped by subspecies (Fig. 4).

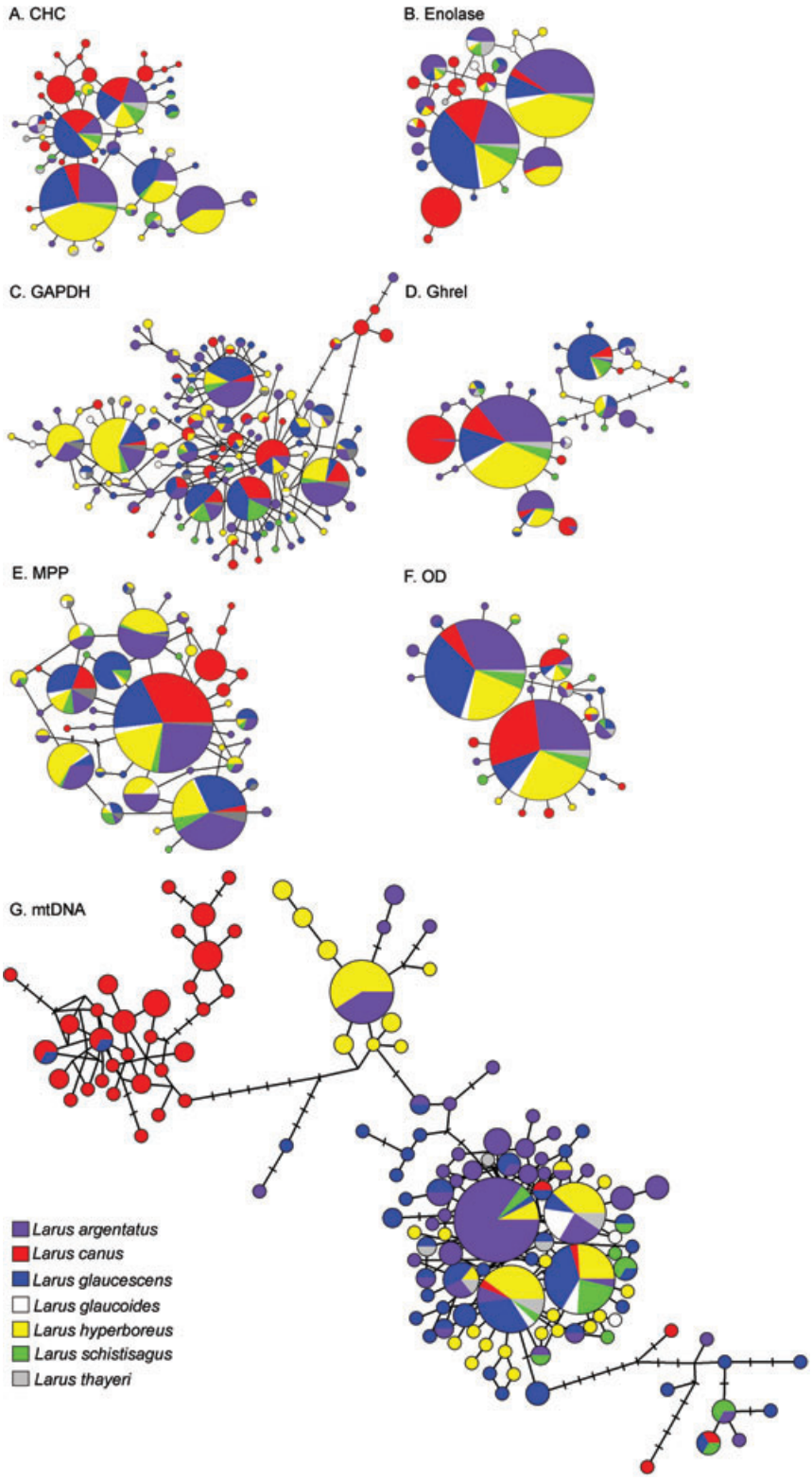

Figure 2. Parsimony networks illustrating relationships of (A) 49 CHC alleles, (B) 24 enolase alleles, (C) 117 GAPDH alleles, (D) 32 ghrel alleles, (E) 42 MPP alleles, (F) 27 OD-7 alleles, and (G) 134 mtDNA control region haplotypes from Arctic gulls, with the size of the circle node corresponding to the frequency of each allele. Each sampled species has a unique color. Tick marks denote unsampled alleles or haplotypes.

Table 2. Overall estimates of population genetic structure (F_{ST}, R_{ST}, and Φ_{ST}) calculated within species with multiple populations and among all species of Arctic gull for 11 microsatellite loci, six nuclear introns, and mtDNA control region. Significant values ($\alpha = 0.05$) are shown in bold text.

	Microsatellites		Introns		mtDNA	
	F_{ST}	R_{ST}	F_{ST}	Φ_{ST}	F_{ST}	Φ_{ST}
Larus argentatus	**0.056**	**0.051**	**0.114**	**0.075**	**0.117**	**0.218**
Larus canus	**0.062**	**0.160**	**0.069**	**0.033**	**0.080**	**0.407**
Larus glaucescens	0.007	**0.048**	**0.074**	0.005	**0.032**	**0.076**
Larus hyperboreus	**0.056**	**0.030**	**0.037**	0.017	**0.537**	**0.160**
Overall	**0.129**	**0.211**	**0.133**	**0.185**	**0.121**	**0.461**

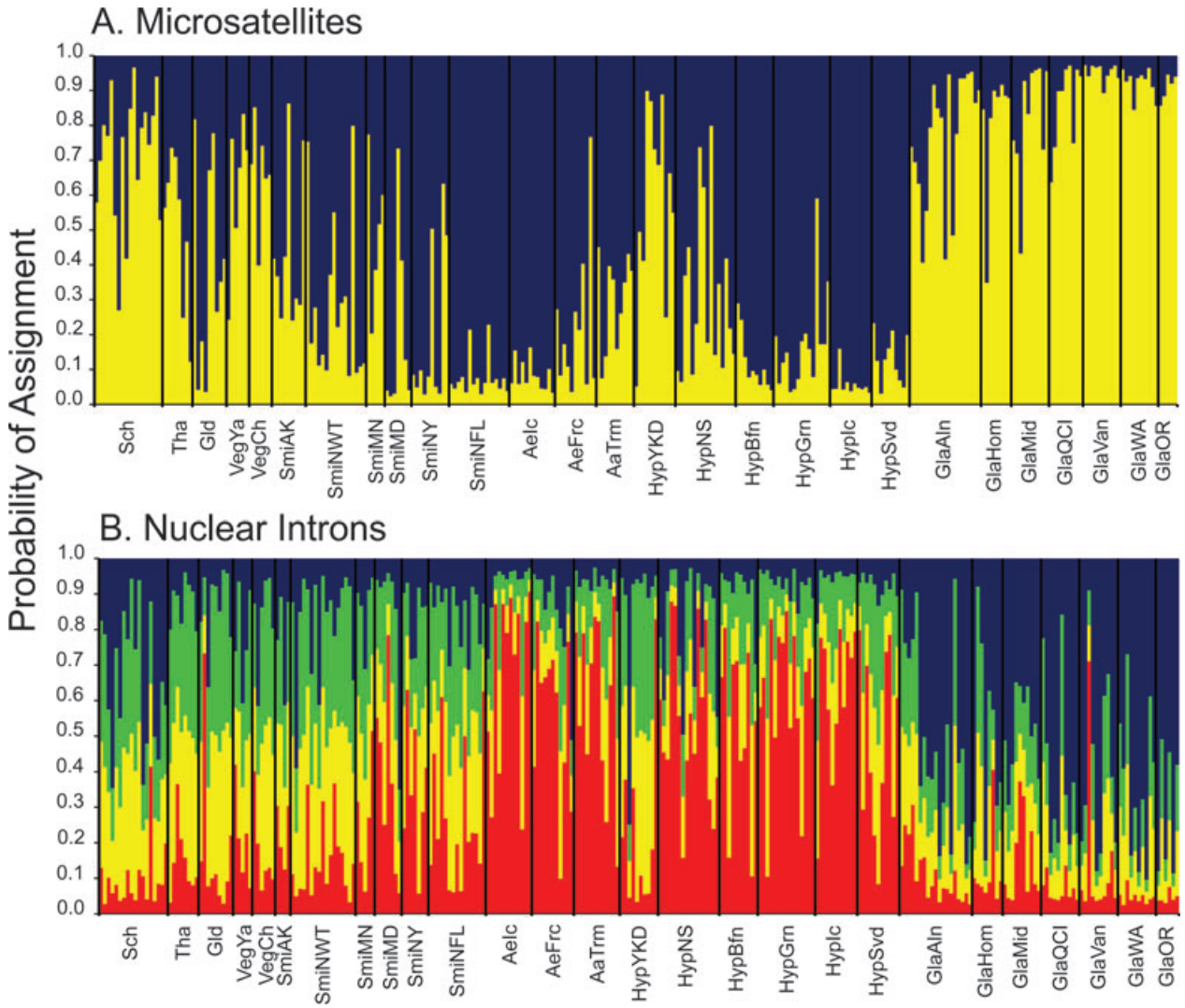

Figure 3. Assignment of Arctic large white-headed gull individuals into (A) two clusters inferred from 11 microsatellite loci and (B) four clusters inferred from six nuclear intron loci in STRUCTURE.

Analyses within species

Variance in microsatellite and nuclear intron allelic frequencies (F_{ST}, R_{ST}, and Φ_{ST}) ranged from 0.030 to 0.114 (Table 2). In contrast to interspecies comparisons, F_{ST} values were typically greater than R_{ST} values for the microsatellite data, with a few exceptions: between northern and southern

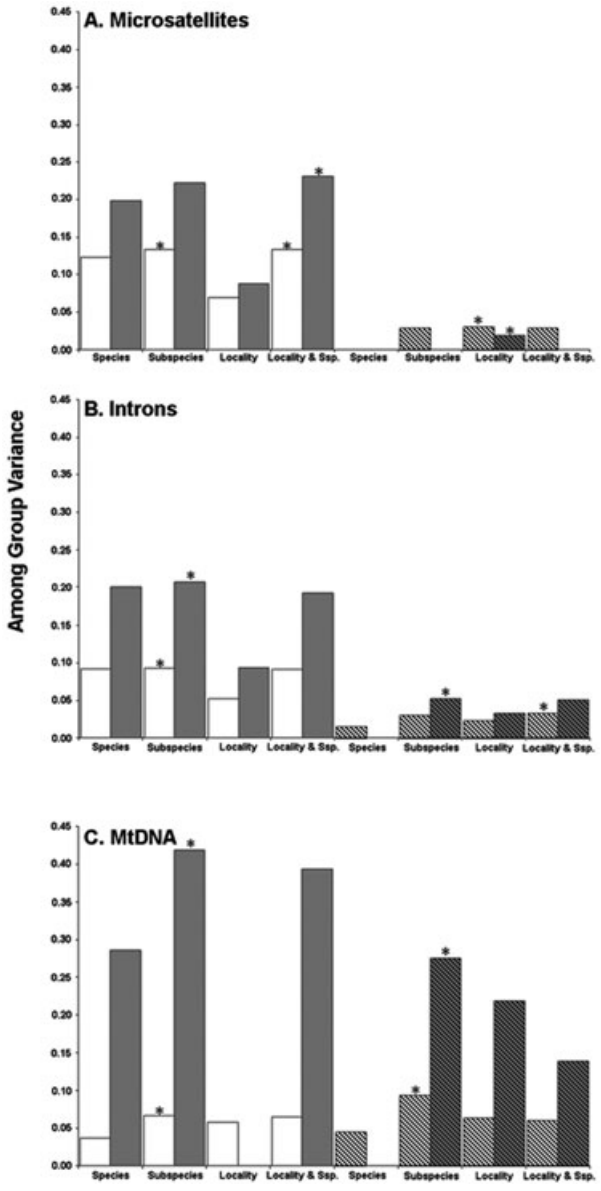

Figure 4. Among group variance (F_{CT}) calculated from (A) 11 microsatellite loci, (B) six nuclear introns, and (C) mtDNA control region for populations grouped to assess the partitioning of genetic variation in Arctic gulls. F_{ST}-based estimates are shown in white and Φ_{ST} based estimates are in gray. Significant F_{CT} values are shown with asterisks denoting population groupings maximizing F_{CT} values. Diagonal bars denote variance estimates based on *Larus argentatus* and *L. hyperboreus* populations only.

populations of *L. glaucescens*, between the *L. argentatus* population from Tromsø and other *L. argentatus* populations, and between populations of *L. canus* from North America and from Russia populations (Appendix S3). However, we observed few significant interpopulation comparisons based on the nuclear intron data (Appendix S3). Variance in mtDNA haplotypic frequencies (F_{ST}) calculated over all populations ranged from 0.080 to 0.537, with larger values observed for most species when the nucleotide substitution model was applied to the data set ($\Phi_{ST} = 0.076$–0.406; Table 2).

Across all within taxa analyses, the likelihood generated for the nuclear intron genotypic data was maximized when K equaled 1. In contrast, genetic partitioning was observed based on microsatellite data. Within *L. argentatus*, ΔK was maximized when K equaled 3 ($\Delta K = 223.7$) (Fig. 5A). *Larus argentatus* individuals from Alaska and Russia clustered together (blue), individuals breeding on the eastern coast of North America grouped together (yellow), and individuals from Iceland, Tromsø, and France clustered together (red) (Fig. 5A). *Larus argentatus* individuals from the Northwest Territories were assigned to the blue and yellow clusters in approximately equal frequencies (Fig. 5A). Within *L. canus*, ΔK was maximized when K equaled 2 ($\Delta K = 368.4$); these two groups corresponded to subspecific classifications, with individuals from North America assigned to one cluster and those from Sweden and Russia to the other (Fig. 5B). ΔK also was maximized when K equaled 2 ($\Delta K = 452.9$) within *L. glaucescens*, although the assignment of individuals did not correspond to sample locality (Fig. 5C). For *L. hyperboreus*, ΔK was maximized when K equaled 4 ($\Delta K = 96.9$) (Fig. 5D). The assignment of individuals appeared to correspond loosely to sample locality, although the signal was not strong; individuals from the Yukon-Kuskokwim Delta were assigned predominately to the green cluster, those from Iceland to the yellow cluster, those from northern Alaska and Baffin Island to the blue cluster, and individuals from Greenland and Svalbard to the red cluster (Fig. 5D).

Population demography

Evidence for significant fluctuations in historical population demography was detected based on microsatellite genotypes. Under the SMM (Table 3), population growth (heterozygote deficiency) was observed for populations of *L. schistisagus* from Kamchatka Peninsula; *L. glaucoides*; *L. argentatus* from Tromsø, France, and Iceland; *L. hyperboreus* from Greenland, Iceland, Chukotka Peninsula, and Yukon-Kuskokwim Delta; *L. glaucescens* from Aleutian Islands, Homer, and Middleton Island; and *L. canus* from south-central Alaska and Northwest Territories. Similar results were observed under the TPM, though fewer populations had signatures of population growth (Table 3).

Significant population growth based on nuclear intron sequences was detected, using LAMARC, for all populations, with theta ($4N_e\mu$) ranging from 0.002 to 0.014 (Table 3). In contrast, all populations had a signal of population stability when g was estimated from mtDNA sequence data, consistent with a pattern of populations located in glacial refugia (Lessa et al. 2004). Theta ($2N_f\mu$) ranged from 0.001 to 4.979

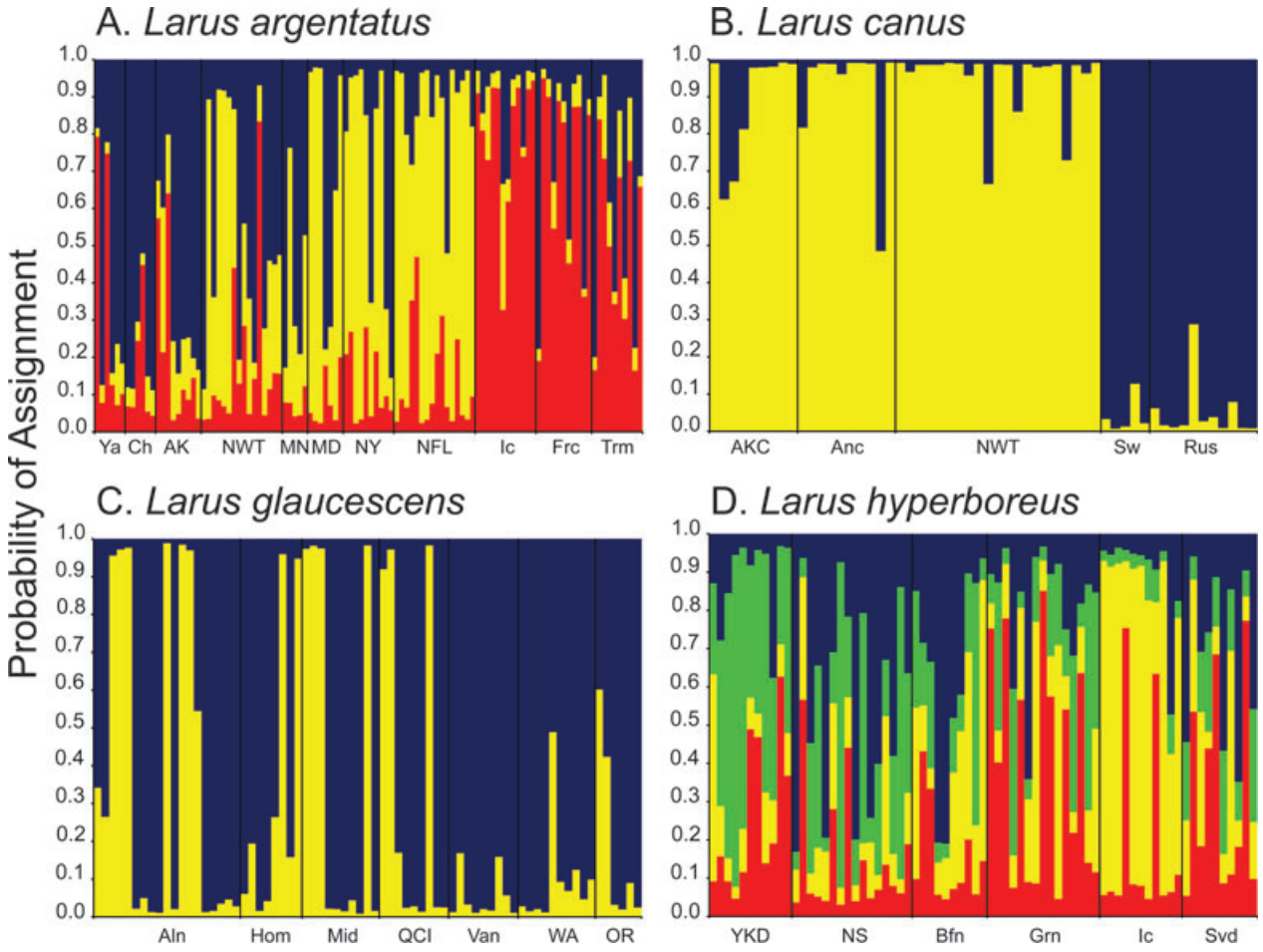

Figure 5. Assignment of (A) *Larus argentatus* individuals into three clusters, (B) *L. canus* individuals into two clusters, (C) *L. glaucescens* individuals into two clusters, and (D) *L. hyperboreus* individuals into four clusters inferred from 11 microsatellite loci in STRUCTURE.

(Table 3). Mismatch distributions estimated from mtDNA sequence data failed to reject the sudden expansion model, based on Harpending's raggedness index (Harpending 1994), for any population. Parameter estimates for time of expansion (τ) ranged from 0.0 to 16.5 (Table 3). The smallest values were observed for populations of *L. hyperboreus* from Iceland, *L. argentatus* from Minnesota, Tromsø, and France, and *L. glaucoides*; the largest estimates for populations of *L. glaucescens* from Middleton Island, *L. hyperboreus* from Greenland, *L. argentatus* from Maryland and Iceland, and *L. canus* from south-central Alaska (Table 3).

Discussion

Multilocus genetic structure within and among species

Despite extensive allele and haplotype sharing among white-headed gull species, genetic substructure was observed within and among species across all marker types. Species and populations at high latitude exhibited lower genetic differentiation then their southern counterparts. Furthermore, individuals breeding at northern latitudes clustered together regardless of species designation, consistent with contemporary hybridization. At least two haplotype/allele groups were observed at each locus; however no haplotype/allele group was represented by a single species at any of the loci. Private alleles and haplotypes were observed for most species at most loci; however, private alleles were only observed in two or three nuclear introns, respectively, for *L. glaucoides* and *L. thayeri* (Fig. 2).

Genetic evidence for contemporary hybridization among northern populations of Arctic white-headed gulls is corroborated by field reports (e.g., *L. glaucescens* × *L. hyperboreus*; *L. argentatus* × *L. hyperboreus*; *L. argentatus* × *L. glaucescens*; *L. glaucescens* × *L. schistisagus*; *L. argentatus* × *L. schistisagus*; *L. glaucoides* × *L. thayeri*; Olsen and Larsson 2004 and

Table 3. Results of demographic analyses for 11 microsatellite loci under the stepwise mutation model (SMM), and two-phased model of mutation (TPM), and for sequence data from six introns and the mitochondrial control region calculated from assayed Arctic gull populations. Parameter estimates θ ($4N_e\mu$ for nuclear DNA, $2N_f\mu$ for mtDNA), exponential growth rate (g), and time of expansion (τ) calculated from mismatch distributions with standard deviations (SD) are provided for each Arctic gull population.

	Microsatellites*		Nuclear introns		mtDNA		
	SMM	TPM	θ	g	θ	g	τ
Sch	H.def.	Eq.	0.014 (0.010–0.021)	892.6 (539.4–943.3)	0.019 (0.007–0.076)	868.4 (−453.2–1031.0)	0.9 (0.3–4.3)
Tha	Eq.	Eq.	0.009 (0.005–0.015)	876.1 (468.7–932.7)	0.015 (0.003–0.147)	912.9 (−66.7–1014.9)	2.4 (0.5–3.3)
Gld	H.def.	H.def.	0.006 (0.004–0.010)	866.8 (385.5–922.5)	0.022 (0.004–7.764)	839.6 (−484.5–990.5)	0.7 (0.0–1.5)
SmiAK	Eq.	Eq.	0.002 (0.001–0.005)	851.3 (174.3–938.7)	0.007 (0.001–0.059)	882.2 (−297.1–1012.0)	3.9 (1.2–6.7)
SmiMD	Eq.	Eq.	0.003 (0.002–0.005)	848.3 (217.8–934.5)	0.065 (0.007–9.030)	845.4 (−468.7–1011.4)	16.5 (3.3–69.5)
SmiMN	Eq.	Eq.	0.003 (0.001–0.008)	849.4 (146.8–935.0)	0.006 (0.001–6.916)	851.3 (−435.8–1020.3)	0.0 (0.0–0.5)
SmiNFL	Eq.	Eq.	0.005 (0.004–0.007)	849.0 (235.2–937.0)	0.010 (0.002–0.057)	850.0 (−398.3–1008.4)	1.1 (0.0–1.9)
SmiNWT	Eq.	Eq.	0.012 (0.011–0.017)	861.3 (321.5–944.0)	0.110 (0.014–8.709)	831.1 (−477.0–997.7)	1.2 (0.2–2.2)
SmiNY	Eq.	Eq.	0.003 (0.002–0.006)	849.9 (173.1–932.6)	0.001 (0.000–0.122)	856.7 (−398.5–1019.6)	3.0 (0.0–50.6)
AaTrm	H.def.	Eq.	0.003 (0.002–0.005)	537.7 (31.4–914.5)	0.006 (0.001–0.020)	753.1 (−426.9–1002.6)	0.0 (0.0–0.0)
AeFrc	H.def.	H.def.	0.002 (0.001–0.005)	843.3 (159.3–930.7)	4.979 (0.021–10.158)	−287.2 (−496.5–956.8)	0.6 (0.0–1.2)
AeIc	H.def.	Eq.	0.003 (0.002–0.005)	862.4 (201.9–938.3)	0.017 (0.006–0.121)	496.0 (−416.7–977.7)	10.9 (6.0–14.7)
VegCh	Eq.	Eq.	0.011 (0.005–0.028)	846.9 (251.3–935.4)	0.011 (0.002–0.411)	784.3 (−472.6–992.0)	2.3 (0.2–11.4)
VegYa	Eq.	Eq.	0.003 (0.002–0.008)	849.9 (123.1–931.8)	0.007 (0.001–1.878)	884.1 (−369.4–1018.4)	6.1 (0.5–9.3)
HypBfn	Eq.	Eq.	0.006 (0.004–0.009)	874.6 (386.9–953.7)	0.010 (0.003–0.085)	868.4 (−410.0–1032.4)	2.9 (0.9–4.9)
HypGrn	H.def.	Eq.	0.005 (0.003–0.008)	861.9 (311.2–942.9)	0.007 (0.002–0.027)	830.8 (−453.8–1000.9)	11.4 (0.12–14.7)
HypIc	H.def.	H.def.	0.002 (0.001–0.004)	866.6 (309.1–948.7)	0.002 (0.001–0.010)	828.3 (−454.5–1007.1)	0.0 (0.0–0.0)
HypRus	H.def.	Eq.	0.004 (0.003–0.007)	869.3 (316.4–946.3)	0.032 (0.009–5.242)	867.4 (−422.8–1030.7)	1.1 (0.0–4.6)
HypSvd	Eq.	Eq.	0.003 (0.003–0.004)	843.5 (216.5–932.1)	0.001 (0.000–0.013)	841.5 (−425.7–1008.5)	2.1 (0.7–4.2)
HypYKD	H.def.	H.def.	0.010 (0.005–0.014)	868.3 (353.5–947.6)	0.017 (0.005–0.216)	880.4 (−365.4–1022.5)	2.3 (0.9–3.5)
GlaAln	H.def.	H.def.	0.005 (0.003–0.009)	814.1 (226.3–926.2)	0.053 (0.015–6.378)	371.4 (−471.8–998.5)	1.2 (0.0–6.2)
GlaHom	H.def.	H.def.	0.006 (0.004–0.012)	846.7 (234.7–937.7)	0.008 (0.001–0.078)	910.9 (−246.1–1013.6)	5.8 (1.4–9.7)
GlaMid	H.def.	H.def.	0.005 (0.005–0.007)	860.5 (300.9–946.2)	1.149 (0.039–9.569)	541.6 (−493.7–971.9)	11.1 (5.1–15.1)
GlaOR	Eq.	Eq.	0.002 (0.001–0.005)	845.6 (936.3–248.1)	0.005 (0.001–0.029)	795.8 (−224.4–1000.3)	2.0 (0.4–3.5)
GlaQCI	Eq.	Eq.	0.002 (0.001–0.003)	850.2 (286.6–940.5)	0.067 (0.012–7.384)	850.2 (−460.2–1031.6)	6.6 (3.3–9.5)
GlaVan	Eq.	Eq.	0.004 (0.004–0.007)	853.2 (166.4–927.5)	0.008 (0.003–0.056)	94.6 (−471.0–919.3)	6.8 (3.1–10.0)

Table 3. Continued

	Microsatellites*		Nuclear introns		mtDNA		
	SMM	TPM	θ	g	θ	g	τ
GlaWA	Eq.	Eq.	0.005 (0.003–0.008)	860.9 (355.7–977.0)	0.025 (0.006–0.308)	238.0 (−428.2–970.2)	2.1 (0.6–6.3)
CanAKC	Eq.	Eq.	0.004 (0.003–0.007)	861.5 (360.3–944.4)	0.065 (0.001–6.146)	−323.4 (−508.7–972.0)	1.1 (0.00–10.1)
CanAnc	H.def.	Eq.	0.004 (0.003–0.008)	871.1 (425.0–950.8)	0.135 (0.018–6.256)	279.5 (−441.2–952.9)	12.9 (5.1–16.7)
CanNWT	H.def.	Eq.	0.007 (0.006–0.008)	865.9 (380.7–946.8)	0.052 (0.019–0.261)	506.9 (−375.7–975.7)	4.1 (2.6–4.9)
CanRus	Eq.	Eq.	0.006 (0.003–0.009)	860.5 (298.7–941.5)	0.006 (0.002–0.025)	835.8 (−422.2–1005.6)	2.5 (0.4–5.4)
CanSw	Eq.	Eq.	0.005 (0.003–0.010)	857.3 (301.2–939.6)	0.001 (0.000–0.014)	839.3 (−366.9–1001.2)	2.3 (0.0–4.3)

*Significant heterozygote deficiency (H.def.) indicates population growth and nonsignificant estimates indicate the population is at equilibrium (Eq).

citations therein). Hybridization would be expected to homogenize allelic frequencies by locality, as neutral loci will remain similar because of introgression and recombination (Mallet 2005). Species appear to have been isolated long enough to have accumulated unique mutations, as indicated by the partitions in the nuclear and mtDNA genomes. Therefore, we contend that hybridization has occurred only recently in Arctic white-headed gull evolutionary history, likely from secondary contact following contemporary range expansion. Introgression of species-specific alleles may be maintained through local adaptation to intermediate habitat types where species coexist, as hybrids have been reported to display adaptive traits of both parental species (*L. glaucescens* × *L. occidentalis*; Good et al. 2000).

Recent speciation and contemporary hybridization likely both play a role in the magnitude of allele and haplotype sharing observed among white-headed gulls. Of particular interest is the extent of introgression/hybridization occurring at the northern limits of species' ranges and among white-headed gulls that breed exclusively at high latitudes. Long-term stable hybrid zones have been reported in temperate areas for several white-headed gull taxa (*L. occidentalis* × *L. glaucescens*, Bell 1996, 1997; Good et al. 2000; *L. argentatus* × *L. marinus*, Crochet et al. 2003) and may be maintained by hybrid superiority at the hybrid zone (Moore 1977). In contrast, white-headed gull species appear to hybridize pervasively throughout northern latitudes (*L. argentatus* × *L. hyperboreus*, Vigfúsdóttir et al. 2008; *L. argentatus* × *L. glaucescens*, Williamson and Peyton 1963; *L. argenatus* × *L. schistisagus*, Olsen and Larsson 2004; *L. glaucoides* × *L. thayeri*, Weir et al. 2000; *L. glaucescens* × *L. schistisagus*, Olsen and Larsson 2004) and discrete hybrid zones appear to be absent. Differences in the degree of hybridization may be attributable to the stability of the habitat where these areas of secondary contact occur. Stable secondary contact zones for gulls are observed at temperate latitudes, where presumably habitat has remained relatively stable throughout the last glacial maximum, allowing species to diverge in allopatry without coming into secondary contact during interglacial periods. Conversely, Arctic species reside in more stochastic environments, where suitable habitat repeatedly contracted and expanded during the Pleistocene glacial cycles (Hewitt 2004). These highly variable climatic conditions likely resulted in a cycle of isolation during glacial periods and secondary contact during interglacial periods, potentially limiting species divergence and development of pre- and postzygotic isolating mechanisms.

Comparatively higher estimates of population structure observed for mtDNA than nuclear DNA markers are consistent with Haldane's rule. Haldane's rule states that hybrids of the heterogametic sex will experience reduced fitness (i.e., greater inviability or sterility) relative to those of the homogametic sex (Coyne and Orr 2004). In birds, females are heterogametic; therefore, if hybrid females were experiencing a strong disadvantage relative to hybrid males, observed genetic differentiation would be greater in mtDNA than nuclear markers. In a study of mainly European white-headed gull populations, researchers proposed that the large discrepancy in interspecific comparisons (mtDNA estimates were 3.3–14.5 times greater than estimates using microsatellites) between marker types could be attributed to a strong disadvantage for hybrid females (Crochet et al. 2003). We did observe high levels of interpopulation comparisons among species for mtDNA ($\Phi_{ST} = 0.130$–0.821; Appendix S3) with no significant comparisons at nuclear markers. However, Haldane's rule would presumably have the greatest influence at secondary contact zones. In these areas, 23% (5/22; Appendix S3) of the comparisons had significant mtDNA

estimates. Of those five, only two comparisons (HypYKD × VegCh, HypIc × AeIc) had proportionally greater degree of divergence than can be explained by differences in the effective population size between genomes (Zink and Barrowclough 2008) and maximum possible F_{ST} value (Meirmans 2006), although differences were slight (HypYKD × VegCh, F_{ST}Exp. = 0.039, F_{ST}Obs. = not significant; HypIc × AeIc, F_{ST}Exp. = 0.051, F_{ST}Obs. = not significant). Therefore, Haldane's rule does not appear to apply to the white-headed gull species studied here.

The lower F_{ST} values observed at nuclear fragment assays (i.e., microsatellites) relative to mtDNA sequence data among species may be attributable to fragment length homoplasy, through not identifying unique alleles because fragments of the same length may have different sequences or may have mutated back to the ancestral state. Both types of homoplasy could pose problems when assessing population structure with fragment analysis based on detecting allelic frequency differences among populations. Most interpopulation comparisons among species have higher R_{ST} than F_{ST} estimates, indicating that the mutation process, and therefore homoplasy, is having an effect on estimators of population subdivision. Caution should be taken when interpreting pairwise population comparisons of allelic variance among species. Rousset (1996) showed that there are no simple effects of homoplasy on estimators of population differentiation (F_{ST} and R_{ST}) for loci evolving under the SMM and island model of migration, making it difficult to assess potential biases in estimates. However, we observed similar signals of population structure based on microsatellite and nuclear intron data. Therefore, the differences in the degree of population structure observed between the genomes studied here may be more attributable to introgression reducing the rate of lineage sorting in the nuclear genome and, to a lesser extent, fragment length homoplasy, although experimental evidence is needed to test this hypothesis.

Pleistocene refugia and comparisons with other taxa

Two distinct mtDNA haplotype groups were observed within *L. argentatus*, *L. canus*, and *L. hyperboreus*, the three sampled taxa with circumpolar distributions, consistent with other studies on white-headed gulls (Fig. 2G; Liebers et al. 2004; Sternkopf et al. 2010). A pattern of at least two allele groups was also observed for the nuclear intron loci (Fig. 2A–F). Concordance in haplotype and allele groups suggests that white-headed gulls were subdivided into at least two refugia that persisted for extended periods of time during the Pleistocene. Furthermore, substructuring observed within mtDNA corresponds to locality. The small central haplotype group is represented by *L. argentatus* individuals from Iceland and Tromsø and *L. hyperboreus* individuals from Iceland, Greenland, Svalbard, and a single individual from northern Alaska (Fig. 2G, population data not shown). All populations of *L. argentatus* are represented in the large haplotype group; however, only North American and Greenland *L. hyperboreus* individuals (and a single individual from Iceland) are observed within this group (Fig. 2G, population data not shown). These findings differ from those of Sternkopf et al. (2010), who identified genetic similarity between *L. hyperboreus* and *L. a. smithsonianus* (the North American subspecies); we did not observe a haplotype group restricted to North America in *L. argentatus*. The presence of a primarily Scandinavian/Greenland/Iceland haplotype group indicates the restriction of at least *L. argentatus* and *L. hyperboreus* into a high-latitude refugium in the North Atlantic/Arctic Ocean, possibly Spitsbergen Bank or northwest Norway. Furthermore, given the restricted geographical distribution of *L. hyperboreus* haplotypes within the central clade, the Scandinavian/Greenland/Iceland refugium was likely isolated from other *L. hyperboreus* populations and did not substantially contribute to the postglacial colonization of North America and Europe.

Despite the presence of species with distributions restricted to northern latitudes, suggestive of restriction to Pleistocene refugia, we were unable to identify glacial refugia for the white-headed gulls studied here based on the coalescent. White-headed gulls are characterized by strong dispersal ability and a propensity to hybridize in areas of secondary contact, as is reflected in contemporary accounts of long-range colonization and subsequent hybridization (Pierotti 1987; Olsen and Larsson 2004; Vigfúsdóttir et al. 2008). The tendency for hybridization at areas of secondary contact is very strong: 16 of the 18 species (89%) are reported to hybridize in nature (Pierotti 1987; Olsen and Larsson 2004 and citations therein) and appear to be free of postzygotic barriers to hybridization (Shields 1987; Snell 1991). Hybridization and subsequent introgression may have erased the genetic legacy of the Pleistocene for white-headed gulls; reductions in effective population sizes associated with the restriction to glacial refugia were not observed, even for populations currently located in glaciated areas. Alternatively, historic Arctic white-headed gull populations that were restricted south and north of the ice sheets likely followed habitat made available by the retreating glacial ice sheets to present day locations. Short movements from refugia would have allowed these historical populations to retain genetic diversity because effective population sizes would not be reduced (Hewitt 1996), especially if colonization occurred over a long period. However, it is unlikely that all populations studied here colonized slowly subsequent to glacial retreat, given the dispersal and colonization ability of Arctic white-headed gulls. Therefore, a more parsimonious explanation is that the strong tendency for hybridization in this group erased the genetic signature of Pleistocene refugia.

Holarctic species typically exhibit shallow but clear phylogeographic signal, due to fragmentation of the distributions of these species into high-latitude glacial refugia, resulting in genetic and morphological differentiation across ranges (Hewitt 2004). Although Arctic white-headed gulls have morphologically distinct forms across their distribution (i.e., subspecies), limited population genetic subdivision among northern Arctic white-headed gull populations was observed. The combination of limited sorting among species (Liebers et al. 2004; Pons et al. 2005) and morphological diversity of taxa, as is evident in gulls, is suggestive of recent allopatric fragmentation and restriction to multiple glacial refugia. Indeed, four populations of gulls (*L. hyperboreus* from Greenland, *L. glaucescens* from Middleton Island, *L. argentatus* from Iceland, and *L. canus* from south-central Alaska) have larger time-of-divergence estimates than other sampled populations and coincide with proposed high-latitude glacial refugia for other taxa (Ploeger 1968). Historical and contemporary hybridization among regions, coupled with small effective population sizes, could have overwhelmed the genetic uniqueness accumulated by northern populations during the last glacial maximum, producing a signal of low genetic structure.

Arctic white-headed gulls are less genetically differentiated at the northern limits of their distribution; this pattern was observed both among species that breed exclusively at high latitudes (*L. schistisagus*, *L. glaucoides*, *L. thayeri*, and *L. hyperboreus*) and within species (e.g., *L. argentatus* and *L. glaucescens*). Liebers and Helbig (2002) observed this pattern between *L. fuscus* and *L. cachinnans*; *L. fuscus* exhibited less genetic structure than its southern counterpart *L. cachinnans*. The authors proposed that differences in the degree of population subdivision indicated that northern gulls are phylogenetically younger than their southern counterparts and were more affected by glacial cycles. In contrast, their southern relatives would have been able to maintain larger long-term stable population sizes during glacial periods. Although Liebers and Helbig's (2002) hypothesis is consistent with observations within Europe, it may not apply to the North American species studied here. In contrast to Europe, high-latitude glacial refugia, notably Beringia, were present in North America during the last glacial maximum and likely promoted genetic diversification in Arctic taxa (Hewitt 2004). As glacial ice sheets retreated, the ranges of temperate species likely expanded northward and came into contact with northern "refugial" populations. Hybridization between "newly arriving" temperate species and northern "refugial" gull species provides an alternate hypothesis for the genetic pattern of decreasing genetic differentiation with increasing latitude.

Arctic white-headed gulls appear to be unique among the Arctic fauna in the spatial distribution of their alleles across species. Previous studies of genetic substructuring among closely related Arctic species reported species-specific clades often correlated with geography (e.g., *Tetraoninae*, Drovetski 2003; *Lemmus* spp., Fedorov et al. 2003; *Motacilla* spp., Pavlova et al. 2003; *Lepus* spp., Waltari and Cook 2005; *Ovis* spp., Loehr et al. 2006; *Riparia* spp., Pavlova et al. 2008). Limited lineage sorting among these seven gull species is noteworthy given that genetic subdivision is regularly observed *within* individual Arctic breeding species (e.g., *Calidris alpina*, Wenink et al. 1996; *Troglodytes troglodytes*, Drovetski 2003; *Rangifer tarandus*, Flagstad and Røed 2003; *Branta canadensis*, Scribner et al. 2003; *Myodes rutilus*, Cook et al. 2004; *Microtus oeconomus*, Galbreath and Cook 2004; *Myopus schisticolor*, Fedorov et al. 2008; *Pinicola enucleator*, Drovetski et al. 2010; *Somateria mollissima*, Sonsthagen et al. 2011). Aspects of white-headed gull behavioral biology, such as colonization ability and propensity to hybridize, as well as their recent evolutionary history, have likely played a large role in the limited genetic structure observed.

Acknowledgments

Funding was provided by the Federal Aviation Administration (FAA) and the Laboratories of Analytical Biology and Division of Birds, National Museum of Natural History, Smithsonian Institution. We thank the following for their significant contributions of tissues for this work: N. Rice, Academy of Natural Sciences of Philadelphia; P. Sweet, American Museum of Natural History; R. Zink and M. Westberg, Bell Museum of Natural History; S. Birks, Burke Museum of Natural History and Culture; D. Boertmann, National Environmental Research Group, Denmark; D. Willard, Field Museum of Natural History; R. Brumfield and D. Dittmann, Louisiana State University Museum of Natural Science; K. Garrett, Natural History Museum of Los Angeles County; J. Dean, National Museum of Natural History; J. Hudon, Royal Alberta Museum; A. Baker and O. Haddrath, Royal Ontario Museum; K. Winker and D. Gibson, University of Alaska Museum; and R. Bowie and C. Cicero, University of California Berkeley Museum of Vertebrate Zoology. We would also like to thank the numerous individuals that helped facilitate field work for the various museums; J. Hunt, Smithsonian Institution, who provided technical laboratory support; C. Milensky and F. Dahlan, Smithsonian Institution, for assistance with sample collection and preparation; and A. Driskell, M. Heacker, and L. Weigt, Smithsonian Institution, K. Omland, University of Maryland Baltimore County, and R. Wilson, University of Alaska Fairbanks, for their guidance and advice throughout this project, as well as two anonymous reviewers comments on earlier drafts of this manuscript. Any use of trade, product, or firm names is for descriptive purposes only and does not imply endorsement by the U.S. Government.

References

Akaike, H. 1974. A new look at the statistical model identification. IEEE Trans. Autom. Control 19:716–723.

Avise, J. C. 2000. Phylogeography: the history and formation of species. Harvard Univ. Press, Cambridge, MA.

Bandelt, H. J., P. Forster, B. C. Sykes, and M. B. Richards. 1995. Mitochondrial portraits of human populations. Genetics 141:743–753.

Banks, R. C., R. T. Chesser, C. Cicero, J. L. Dunn, A. W. Kratter, I. J. Lovette, P. C. Rasmussen, J. V. Remsen, Jr., J. D. Rising, D. F. Stotz, *et al*. 2008. Forty-ninth supplement to the American Ornithologists Union check-list of North American birds. Auk 125:758–768.

Bell, D. A. 1996. Genetic differentiation, geographic variation and hybridization in gulls of the *Larus glaucescens–occidentalis* complex. Condor 98:527–546.

Bell, D. A. 1997. Hybridization and reproductive performance in gulls of the *Larus glaucescens–occidentalis* complex. Condor 99:585–594.

Cook, J. A., A. M. Runck, and C. J. Conroy. 2004. Historical biogeography at the crossroads of the northern continents: molecular phylogenetics of red-backed voles (Rodentia: Arvicolinae). Mol. Phylogenet. Evol. 30:767–777.

Cornuet, J. M., and G. Luikart. 1996. Description and power analysis of two tests for detecting recent population bottlenecks from allele frequency data. Genetics 144:2001–2014.

Coyne, J. A., and H. A. Orr. 2004. Speciation. Sinauer Associates, Sunderland, MA.

Crochet, P.-A., J. Z. Chen, J.-M. Pons, J.-D. Lebreton, P. D. N. Hebert, and F. Bohnomme. 2003. Genetic differentiation at nuclear and mitochondrial loci among large white-headed gulls: sex-biased interspecific gene flow? Evolution 57:2865–2878.

DeWoody, J. A., J. Schupp, L. Kenefic, J. Busch, L. Murfitt, and P. Keim. 2004. Universal method for producing ROX-labeled size standards suitable for automated genotyping. BioTechniques 37:348–352.

Drovetski, S. V. 2003. Plio-Pleistocene climatic oscillations, Holarctic biogeography and speciation in an avian subfamily. J. Biogeogr. 30:1173–1181.

Drovetski, S. V., R. M. Zink, P. G. P. Ericson, and I. V. Fadeev. 2010. A multilocus study of pine grosbeak phylogeography supports the pattern of greater intercontinental divergence in Holarctic boreal forest birds than in birds inhabiting other high-latitude habitats. J. Biogeogr. 37:696–706.

Evanno, G., S. Regnaut, and J. Goudet. 2005. Detecting the number of clusters of individuals using the software STRUCTURE: a simulation study. Mol. Ecol. 14:2611–2620.

Excoffier, L., P. E. Smouse, and J. M. Quatro. 1992. Analysis of molecular variance from metric distances among DNA haplotypes: applications to human mitochondrial DNA restriction data. Genetics 131:479–491.

Fedorov, V., A. V. Goropashnaya, M. Jaarola, and J. A. Cook. 2003. Phylogeography of lemmings (*Lemmus*): no evidence for postglacial colonization of Arctic from the Beringian refugium. Mol. Ecol. 12:725–731.

Fedorov, V., A. V. Goropashnaya, G. G. Boeskorov, and J. A. Cook. 2008. Comparative phylogeography and demographic history of the wood lemming (*Myopus schisticolor*): implications for late Quaternary history of the taiga species in Eurasia. Mol. Ecol. 17:598–610.

Flagstad, Ø., and K. H. Røed. 2003. Refugial origins of reindeer (*Rangifer tarandus* L.) inferred from mitochondrial DNA sequences. Evolution 57:658–670.

Fluxus Technology Ltd. 2008. NETWORK 4.5.1.0. Distributed over the internet. Available at http://www.fluxus-engineering.com. Accessed February 1, 2009.

Galbreath, K. E., and J. A. Cook. 2004. Genetic consequences of Pleistocene glaciations for the tundra vole (*Microtus oeconomus*) in Beringia. Mol. Ecol. 13:135–148.

Gay, L., G. Neubauer, M. Zagalska-Neubauer, C. Bebain, J.-M. Pons, P. David, and P.-A. Crochet. 2007. Molecular and morphological patterns of introgression between two large white-headed gull species in a zone of recent secondary contact. Mol. Ecol. 16:3215–3227.

Given, A. D., J. A. Mills, and A. J. Baker. 2002. Isolation of polymorphic microsatellite loci from the red-billed gull (*Larus novaehollandiae scopulinus*) and amplification in related species. Mol. Ecol. Notes 2:416–418.

Good, T. P., J. C. Ellis, C. A. Annett, and R. Pierottie. 2000. Bounded hybrid superiority in an avian hybrid zone: effects of mate, diet, and habitat choice. Evolution 54:1774–1783.

Goudet, J. 1995. FSTAT vers. 1.2: a computer program to calculate *F*-statistics. J. Hered. 86:485–486.

Gregory, S. M., and J. S. Quinn. 2006. Microsatellite isolation from four avian species comparing two isolation techniques. Mol. Ecol. Notes 6:87–89.

Harpending, R. C. 1994. Signature of ancient population growth in a low-resolution mitochondrial DNA mismatch distribution. Hum. Biol. 66:591–600.

Harrigan, R. J., M. E. Mazza, and M. D. Sorenson. 2008. Computation vs. cloning: evaluation of two methods for haplotype determination. Mol. Ecol. Res. 8:1239–1248.

Hedrick, P. W. 2005. A standardized genetic differentiation measure. Evolution 59:1633–1638.

Hewitt, G. M. 1996. Some genetic consequences of ice ages, and their role in divergence and speciation. Biol. J. Linn. Soc. 58:247–276.

Hewitt, G. M. 2000. The genetic legacy of the Quaternary ice ages. Nature 405:907–913.

Hewitt, G. M. 2001. Speciation, hybrid zones and phylogeography—or seeing genes in space and time. Mol. Ecol. 10:537–549.

Hewitt, G. M. 2004. Genetic consequences of climatic oscillations in the Quaternary. Philos. Trans. R. Soc. Lond. B. Biol. Sci. 359:183–195.

Kuhner, M. K. 2006. LAMARC 2.0: maximum likelihood and Bayesian estimation of population parameters. Bioinformatics 22:768–770.

Kuhner, M. K., and L. P. Smith. 2007. Comparing likelihood and Bayesian coalescent estimation of population parameters. Genetics 175:155–165.

Lessa, E. P., J. A. Cook, and J. L. Patton. 2004. Genetic footprints of demographic expansion in North America, but not Amazonia, during the Late Quaternary. Proc. Natl. Acad. Sci. USA 100:10331–10334.

Liebers, D., and A. J. Helbig. 2002. Phylogeography and colonization history of lesser black-backed gulls (*Larus fuscus*) as revealed by mtDNA sequences. J. Evol. Biol. 15:1021–1033.

Liebers, D., A. J. Helbig, and P. de Kniff. 2001. Genetic differentiation and phylogeography of gulls in the *Larus cachinnans-fuscus* group (Aves: Charadriiformes). Mol. Ecol. 10:2447–2462.

Liebers, D., P. de Kniff, and A. J. Helbig. 2004. The herring gull complex is not a ring species. Proc. R. Soc. Lond. B 271:893–901.

Loehr, J., K. Worley, A. Grapputo, J. Carey, A. Veitch, and D. W. Coltman. 2006. Evidence for cryptic glacial refugia from North American mountain sheep mitochondrial DNA. J. Evol. Biol. 19:419–430.

Mallet, J. 2005. Hybridization as an invasion of the genome. Trends Ecol. Evol. 20:292–237.

Meirmans, P. G. 2006. Using the AMOVA framework to estimate a standardized genetic differentiation measure. Evolution 60:2399–2402.

Moore, W. S. 1977. An evaluation of narrow hybrid zones in vertebrates. Q. Rev. Biol. 52:263–277.

Olsen, K. M., and H. Larsson. 2004. Gulls of North America, Europe, and Asia. Princeton Univ. Press, New Jersey.

Pavlova, A., R. M. Zink, S. V. Drovetski, Y. Redkin, and S. Rohwer. 2003. Phylogeographic patterns in *Motacilla flava* and *Motacilla citreola*: species limits and population history. Auk 120:774–758.

Pavlova, A., R. M. Zink, S. V. Drovetski, and S. Rohwer. 2008. Pleistocene evolution of closely related sand martins *Riparia riparia* and *R. diluta*. Mol. Phylogenet. Evol. 48:61–73.

Pierotti, R. 1987. Isolating mechanisms in seabirds. Evolution 41:559–570.

Ploeger, P. L. 1968. Geographical differentiation in arctic Anatidae as a result of isolation during the last glacial period. Ardea 56:1–159.

Pons, J.-M., A. Hassanin, and P.-A. Crochet. 2005. Phylogenetic relationships within the *Laridae* (Charadriiformes: *Aves*) inferred from mitochondrial markers. Mol. Phylogenet. Evol. 37:686–699.

Posada, D., and K. A. Crandall. 1998. Modeltest: testing the model of DNA substitution. Bioinformatics 14:817–818.

Pritchard, J. K., M. Stephens, and P. Donnelly. 2000. Inference of population structure from multilocus genotype data. Genetics 155:945–959.

Rogers, A. R., and H. Harpending. 1992. Population growth makes waves in the distribution of pairwise genetic differences. Mol. Biol. Evol. 9:552–569.

Rousset, F. 1996. Equilibrium values of measures of population subdivision for stepwise mutation processes. Genetics 142:1357–1362.

Schafer, A. B., C. I. Cullingham, S. D. Cote, and D. W. Coltman. 2010. Of glaciers and refugia: a decade of study sheds new light on the phylogeography of northwestern North America. Mol. Ecol. 19:4589–4621.

Schmitt, T. 2007. Molecular biogeography of Europe: Pleistocene cycles and postglacial trends. Front. Zool. 4:11.

Schneider, S., D. Roessli, and L. Excoffier. 2000. ARLEQUIN ver. 2.0: a software for population genetic data analysis. Genetics and Biometry Laboratory, University of Geneva, Geneva.

Scribner, K. T., S. L. Talbot, J. M. Pearce, B. J. Pierson, K. S. Bollinger, and D. V. Derksen. 2003. Phylogeography of Canada geese (*Branta canadensis*) in Western North America. Auk 120:889–907.

Shields, G. F. 1987. Chromosomal variation. Pp. 79–104 *in* F. Cooke and P. A. Buckley, eds. Avian genetics: a population and ecological approach. Academic Press, New York.

Snell, R. R. 1991. Interspecific allozyme differentiation among North-Atlantic white-headed Larid gulls. Auk 108:319–328.

Sonsthagen, S. A., S. L. Talbot, and K. G. McCracken. 2007. Genetic characterization of common eiders (*Somateria mollissima*) breeding in the Yukon Kuskokwim Delta, Alaska. Condor 109:879–894.

Sonsthagen, S. A., S. L. Talbot, K. T. Scribner, and K. G. McCracken. 2011. Multilocus phylogeography and population structure of common eiders breeding in North America and Scandinavia. J. Biogeogr. 38:1368–1380.

Stephens, M., N. Smith, and P. Donnelly. 2001. A new statistical method for haplotype reconstruction from population data. Am. J. Hum. Genet. 68:978–989.

Sternkopf, V., D. Liebers-Helbig, M. S. Ritz, J. Zhang, A. J. Helbig, and P. de Knijff. 2010. Introgressive hybridization and the evolutionary history of the herring gull complex revealed by mitochondrial and nuclear DNA. BMC Evol. Biol. 10:348.

Tajima, F. 1989. The effect of change in population size on DNA polymorphism. Genetics 123:597–601.

Tirard, C., F. Helfenstein, and E. Danchin. 2002. Polymorphic microsatellites in the black-legged kittiwake *Rissa tridactyla*. Mol. Ecol. Notes 2:431–433.

Velichko, A. A., Y. M. Kononov, and M. A. Faustova. 1997. The last glaciation of Earth: Size and volume of ice-sheets. Quatern. Int. 41–42:43–51.

Vigfúsdóttir, F., S. Pálsson, and A. Ingólfsson. 2008. Hybridization of glaucous gull (*Larus hyperboreus*) and herring gull (*Larus argentatus*) in Iceland: mitochondrial and microsatellite data. Philos. Trans. R. Soc. B 363:2851–2860.

Waltari, E., and J. A. Cook. 2005. Hares on ice: phylogeography and historical demographics of *Lepus arcticus*, *L. othus*, and *L. timidus* (Mammalia: Lagomorpha). Mol. Ecol. 14:3005–3016.

Weir, D. N., A. C. Kitchener, and R. Y. McGowan. 2000. Hybridization and changes in the distribution of Iceland gulls (*Larus glaucoides/kumlieni/thayeri*). J. Zool. 252:517–530.

Wenink, P. W., A. J. Baker, H.-U. Rosner, and M. G. J. Tilanus. 1996. Global mitochondrial DNA phylogeography of Holarctic breeding dunlins (*Calidris alpina*). Evolution 50:318–330.

Williams, M., D. Dunkerley, P. De Deckker, P. Kershaw, and J. Chappel. 1998. Quaternary Environments. Oxford Univ. Press, New York.

Williamson, F. S. L., and L. J. Peyton. 1963. Interbreeding of glaucous-winged and herring gulls in the Cook Inlet Region, Alaska. Condor 65:24–28.

Zink, R. M., and G. F. Barrowclough. 2008. Mitochondrial DNA under siege in avian phylogeography. Mol. Ecol. 17:2107–2121.

Supporting Information

Additional Supporting Information may be found online on Wiley Online Library.

Appendix S1. Collection localities and museum catalogue number for museum voucher specimens used in this study.
Appendix S2. Primer sequences, PHASE and MODELTEST results for assayed nuclear intron and mtDNA control region loci.
Appendix S3. Interpopulation F_{ST}, R_{ST}, and Φ_{ST} values calculated among Arctic gull populations.

Please note: Wiley-Blackwell is not responsible for the content or functionality of any supporting materials supplied by the authors. Any queries (other than missing material) should be directed to the corresponding author for the article.

Appendix S1. Collection localities and museum* catalogue number for museum voucher specimens used in this study, with population abbreviations in parentheses.

Larus argentatus argentatus

Norway: Tromsø (Trm)

ROM RRS 407, ROM RRS 408, ROM RRS 409, ROM RRS 411, ROM RRS 412, ROM RRS 413, ROM RRS 418, ROM RRS 419, ROM RRS 420, ROM RRS 421

Larus argentatus argenteus

France: Finistere, Ile de Balanec (Frc)

ROM RRS 567, ROM RRS 569, ROM RRS 570, ROM RRS 572, ROM RRS 574, ROM RRS 574, ROM RRS 575, ROM RRS 576, ROM RRS 577, ROM RRS 578

Iceland (Ic)

ROM RRS 291, ROM RRS 292, ROM RRS 294, ROM RRS 296, ROM RRS 325, ROM RRS 327, ROM RRS 331, ROM RRS 332, ROM RRS 334, ROM RRS 336, USNM 627643, USNM 627675

United Kingdom (Frc)

DOT 11128, USNM 621344

Larus argentatus smithsonianus

Canada: Alberta, Bonnyville (NWT)

USNM 641400, USNM 641402, USNM 641403

Canada: Alberta, Lac La Biche (NWT)

USNM 641377

Canada: Newfoundland (NFL)

USNM 637965, USNM 637966, USNM 637967, USNM 637968, USNM 637969,

USNM 637970, USNM 637971

Canada: Northwest Territories, Great Slave Lake (NWT)

RAM 32696, RAM 32697, RAM 32698, RAM 32699, RAM 32700, RAM 32701, RAM 32702, RAM 32703, RAM 32704, RAM 32705, RAM 32706, RAM 32707

Canada: Prince Edward Island (NFL)

ROM RRS 340, ROM RRS 341, ROM RRS 342, ROM RRS 352, ROM RRS 355, ROM RRS 356, ROM RRS 360, ROM RRS 368

USA: Alaska (AK)

UAM 7725, UWBM 53950, UWBM 53951, UWBM 53953

USA: Illinois (MN)

FMNH 438242

USA: Maryland (MD)

USNM 636189, USNM 638657, USNM 638658, USNM 638659, USNM 638688, USNM 638685, USNM 638687

USA: Minnesota (MN)

BMNH 42558, FMNH 388020, FMNH 396981

USA: New Jersey (NY)

ANSP 7269

USA: New York (NY)

DOT 10245, DOT 10247, DOT 10248, DOT 10250, DOT 10252, USNM 641186

USA: Wisconsin (MN)

FMNH 441565

Larus argentatus vegae

Russia: Chukoskiy Avtonomnyy Okrug (Ch)

BMNH 44781, UWBM 43911, UWBM 43983,

Russia: Primorskiy Kray, Spasskiy Rayon (Ch)

UWBM 71997

Russia: Tyumenskaya Oblast', Yamalo-Nenetskiy Avtonomnyi Okrug (Ya)

UWBM 56728, UWBM 56820, UWBM 56821, UWBM 56826, UWBM 59530,

UWBM 59584

USA: Alaska, Norton Sound (Ch)

UAM 13016

USA: Alaska, Shemya (Ch)

UAM 9410

Larus canus brachyrhynchus

Canada: Northwest Territories, Great Slave Lake (NWT)

ROM DL 419, ROM DL 420, ROM DL 421, ROM DL 422, ROM DL 423, ROM DL

424, ROM DL 425, ROM DL 426, ROM DL 427, ROM DL 428, RAM 32736, RAM

32737, RAM 32738, RAM 32739, RAM 32740, RAM 32741, RAM 32742, RAM

32743, RAM 42744, RAM 32745, RAM 32750

USA: Alaska, Central (AKC)

BMNH 41347, BMNH 41372, LSUMZ 36853, LSUMZ 36854, LSUMZ 36855,

UWBM 53885, UWBM 53949, UWBM 53964, UWBM 54037

USA: Alaska, Southcentral (Anc)

ANSP 1771, BMNH 38654, USNM 601795, USNM 622481, USNM 627778, USNM

638719, USNM 638795, USNM 638796, USNM 638797, USNM 638798

Larus canus canus

Sweden (Sw)

LSUMZ 12233, LSUMZ 12234, LSUMZ 12239

United Kingdom (Sw)

DOT 10848, USNM 627553

Larus canus kamtschatschensis

Russia: Kamchatka (Rus)

BMNH 44728, UWBM 44049, UWBM 44068, UWBM 44309, UWBM 44333, UWBM 44334, UWBM 44335, UWBM 44336, UWBM 44337, UWBM 44338, UWBM 44339

Larus glaucescens

Canada: British Columbia, Queen Charlotte Island (QCI)

MVZ 172540, MVZ 172542, MVZ 172546, MVZ 172548, MVZ 172552, MVZ 172553, MVZ 172555, MVZ 172556, MVZ 172557

Canada: British Columbia, Vancouver Island (Van)

MVZ 172623, MVZ 172624, MVZ 172626, MVZ 172627, MVZ 172640, MVZ 172641, MVZ 172642, MVZ 172645, MVZ 172648

USA: Alaska, Aleutian Islands (Aln)

BMNH 38644, BMNH 38645, BMNH 38657, BMNH 38658, DOT 1154, DOT 1155, DOT 1156, DOT 1157, DOT 1158, MVZ 172500, MVZ 172501, MVZ 172502, MVZ 172503, MVZ 172504, USNM 638721, USNM 638722, USNM 627780, USNM 627782, USNM 627783

USA: Alaska, Kachemak Bay, Homer (Hom)

MVZ 172505, MVZ 172506, MVZ 172507, MVZ 172508, MVZ 172509, MVZ

172510, MVZ 172511, MVZ 172512

USA: Alaska, Middleton Island (Mid)

MVZ 172519, MVZ 172520, MVZ 172521, MVZ 172522, MVZ 172523, MVZ

172524, MVZ 172525, MVZ 172526, MVZ 172527, MVZ 172529

USA: Oregon (OR)

MVZ 172723, MVZ 172724, MVZ 172725, MVZ 172726, MVZ 172727, MVZ 172728

USA: Washington (WA)

MVZ 172667, MVZ 172669, MVZ 172671, MVZ 172672, MVZ 172674, MVZ

172710, MVZ 172711, MVZ 172714, MVZ 172715, MVZ 172716

Larus glaucoides kumlieni

Canada: Nunuvat, Baffin Island

ROM RRS 102, ROM RRS 105, ROM RRS 106, ROM RRS 109, ROM RRS 110,

ROM RRS 123, ROM RRS 137, ROM RRS 163, USNM 637972

Larus hyperboreus barrovianus

USA: Alaska, Arctic Ocean (NS)

UWBM 72704, UWBM 72705, UWBM 72706, UWBM 72707, UWBM 72708,

UWBM 72709, UWBM 72710, UWBM 72712, UWBM 72713, UWBM 72714

USA: Alaska, North Slope Borough (NS)

UWBM 79180, UWBM 79186

USA: Alaska, Yukon-Kuskokwim Delta (YK)

ROM TB 9501, ROM TB 9503, ROM TB 9505, ROM TB 9510, ROM TB 9511, ROM

TB 9513, ROM TB 9516, ROM TB 9519, ROM TB 9522, USNM 627779, USNM

638720

Larus hyperboreus hyperboreus

Canada: Newfoundland (Bfn)

USNM 637973

Canada: Nunuvat, Baffin Island (Bfn)

ROM RRS 103, ROM RRS 112, ROM RRS 113, ROM RRS 118, ROM RRS 125,

ROM RRS 128, ROM RRS 129, ROM RRS 130, ROM RRS 161, ROM RRS 167

Greenland: Scoresbysund (Grn)

Hyp 1, Hyp 2, Hyp 3, Hyp 4, Hyp 5, Hyp 6, Hyp 7, Hyp 8, Hyp 9, Hyp 10, Hyp 11, Hyp

12, Hyp 13, Hyp 14, Hyp 15

Iceland: Bjarnarhafnarfjall (Ic)

ROM RRS 208, ROM RRS 209, ROM RRS 211, ROM RRS 216, ROM RRS 219,

ROM RRS 220, ROM RRS 221, ROM RRS 222, ROM RRS 223, ROM RRS 224

Norway: Spitsbergen, Svalbard Arch (Svd)

ROM RRS 472, ROM RRS 474, ROM RRS 477, ROM RRS 478, ROM RRS 480,

ROM RRS 481, ROM RRS 482, ROM RRS 483, ROM RRS 484, ROM RRS 490

Larus hyperboreus pallidissimus

Russia: Chukotskiy Avtonomnyy Okrug (NS)

UWBM 43982

Russia: Magadanskaya Oblast' (NS)

UWBM 43851, UWBM 43852, UWBM 43853

Larus schistisagus

Russia: Kamchatka

UWBM 44050, UWBM 44340, UWBM 44341

Russia: Magadanskaya Oblast', Magadan

UWBM 43821, UWBM 43822, UWBM 43847, UWBM 43848, UWBM 44183,

UWBM 44185, UWBM 44186, UWBM 44187, UWBM 44188, UWBM 44189

Russia: Sakhalinskaya Oblast', Sakhalin

UWBM 47275, UWBM 47299, UWBM 47276

USA: Alaska

UAM 13155, UAM 10022

Larus thayeri

Canada: Nunuvat, Home Bay Island

ROM RRS 124, ROM RRS 127

Canada: Ontario

ROM 1B-1755, ROM 1B-4507

USA: California

LAF 6596

USA: California, Monterey Bay

MVZ 175953, MVZ 175954, MVZ 175955

---

* Museum abbreviations: ANSP = Academy of Natural Sciences of Philadelphia, BMNH = Bell Museum of Natural History, DOT = American Museum of Natural History, FMNH = Field Museum of Natural History, LAF = Natural History Museum of Los Angeles County, LSUMZ = Louisiana State University Museum of Natural Science, MVZ = University of California Berkeley Museum of Vertebrate Zoology, RAM = Royal Alberta Museum, ROM = Royal Ontario Museum, UAM = University of Alaska Museum, USNM = National Museum of Natural History, and UWBM = Burke Museum of Natural History and Culture. Specimen numbers

prefixed with Hyp were provided from a private research collection (Dr. David Boertmann, University of Aarhus, Denmark).

Appendix S2. Sequence length, primers, number of variable sites, number of reconstructed alleles, observed homozygosity, background recombination rate (ρ), factors exceeding the ρ estimated in PHASE, and the nucleotide substitution model that best fit the sequence data determined in MODELTEST for each of the six nuclear introns and mtDNA control region assayed for seven species of Arctic white-headed gulls.

	Length	Primers (5'–3')[1]	Variable Sites	Alleles	H_o	ρ	Factors Exceeding ρ	Model[2]
CHC	664–665	CHC5F (GCCCCAAAGGTAATAGACTGG): CHC6R (GCGTATGGTGTCTGGAGTACGC)	41	49	75.4	0.002	0.627–1.534	HKY+I+G
Enolase	330–331	EnolL731:EnolH912	15	24	60.7	0.011	0.359–2.515	HKY+I+G
GAPDH	419–423	G3P13F:GAPDH.12R	46	117	63.6	0.053	0.486–1.723	GTR+I+G
Ghrel	519–528	Ghrel3F (GCAACAATCTAAAGTGTATTTAGG): Ghrel4R (TCTTGACACCAATTTCAAARGGAAC) Ghrel-IntF (GCAACAATCTAAAGTGTATTTAGG): Ghrel-IntR (CCATCTATTCACTTAGCGC)	30	32	39.2	0.003	0.625–1.678	K81uf+I
MPP	323–324	MPP4.F:MPP5.R	28	42	69.8	0.096	0.626–1.435	TVM+I
OD7	390	OD7F:OD7R	21	27	59.3	0.000	0.633–1.808	K81uf+G

mtDNA	392	L15522 (GACTTAYGGCCYGAAAAGCC): H1816 and H419:H519	54	134	–	–	–	GTR+I+G

[1]Published primers were used for Enolase (Friesen *et al.*, 1997), GAPDH (Van Tuinen *et al.*, 2001; Sonsthagen *et al.*, 2007), MPP (Friesen *et al.*, 1999), and OD7 (Sonsthagen *et al.*, 2007), and mtDNA (Helbig & Seibold, 1999; Liebers *et al.*, 2001).

[2]Model abbreviations: I = invariant site parameter, G = rate variation among sites, GTR = General time reversible (Tavaré 1986), HKY = Hasegawa, Kishino, Yano 85 (Hasegawa *et al.*, 1985), K81uf = two transversion-parameters model 1 with unequal frequencies (Kimura, 1981), and TVM = transversional model (Posada & Crandall, 1998).

Appendix S3. Interpopulation F_{ST}, R_{ST}, and Φ_{ST} values calculated from 11 microsatellite loci, six nuclear intron loci, and mtDNA control region for Arctic white-headed gull populations.

	µsat – F_{ST}	µsat – R_{ST}	mtDNA – Φ_{ST}	Introns – Φ_{ST}
Sch				
–Tha	0.015	**0.073**	0.062	-0.005
–Gld	**0.040**	0.016	**0.084**	0.021
–VegYa	0.024	-0.107	0.182	-0.064
–VegCh	0.010	-0.024	-0.027	0.007
–SmiAK	0.022	0.043	0.007	-0.048
–SmiNWT	**0.054**	**0.102**	**0.175**	-0.021
–SmiMN	0.023	-0.122	0.009	0.078
–SmiMD	**0.093**	**0.091**	0.144	0.049
–SmiNY	**0.101**	**0.080**	**0.228**	0.067
–SmiNFL	**0.133**	**0.119**	**0.285**	0.000
–AeIc	**0.104**	**0.091**	**0.261**	**0.208**
–AeFrc	**0.105**	**0.107**	**0.146**	0.026
–AaTrm	**0.075**	**0.120**	**0.402**	**0.181**
–HypNS	**0.081**	**0.095**	0.049	**0.075**
–HypYKD	**0.029**	0.047	0.063	0.034
–HypBfn	**0.107**	**0.154**	0.071	**0.082**
–HypGrn	**0.092**	**0.140**	**0.141**	**0.092**
–HypIc	**0.182**	**0.107**	**0.594**	**0.259**
–HypSvd	**0.125**	**0.128**	**0.621**	0.054

–GlaAln	**0.030**	0.020	-0.032	0.026
–GlaHom	0.016	-0.004	0.037	0.022
–GlaMid	**0.033**	**0.061**	0.076	**0.078**
–GlaQCI	**0.044**	**0.092**	**0.188**	**0.065**
–GlaVan	**0.052**	**0.148**	0.041	0.058
–GlaWA	**0.048**	**0.178**	-0.017	**0.078**
–GlaOR	**0.053**	**0.278**	0.025	0.030
–CanRus	**0.117**	**0.125**	**0.661**	**0.262**
–CanAKC	**0.116**	**0.278**	**0.483**	**0.241**
–CanAnc	**0.157**	**0.324**	**0.399**	**0.147**
–CanNWT	**0.145**	**0.297**	**0.656**	**0.047**
–CanSw	**0.221**	**0.200**	**0.729**	**0.116**
Tha				
–Gld	0.023	0.099	-0.010	0.026
–VegYa	**0.061**	-0.107	**0.260**	0.061
–VegCh	0.033	-0.119	0.076	-0.051
–SmiAK	0.022	0.008	0.025	-0.106
–SmiNWT	0.026	**0.085**	**0.188**	**0.093**
–SmiMN	0.010	-0.169	**0.218**	**0.123**
–SmiMD	**0.090**	**0.136**	**0.218**	**0.180**
–SmiNY	**0.120**	**0.103**	**0.457**	**0.173**
–SmiNFL	**0.140**	**0.254**	**0.434**	**0.102**
–AeIc	**0.081**	**0.152**	**0.351**	**0.268**

–AeFrc	**0.100**	0.143	**0.201**	**0.104**
–AaTrm	**0.056**	**0.129**	**0.528**	**0.240**
–HypNS	**0.056**	**0.133**	0.012	**0.134**
–HypYKD	**0.022**	0.030	0.053	**0.095**
–HypBfn	**0.077**	**0.160**	0.068	**0.153**
–HypGrn	**0.083**	**0.202**	0.148	**0.145**
–HypIc	**0.165**	**0.196**	**0.788**	**0.327**
–HypSvd	**0.092**	0.067	**0.816**	**0.137**
–GlaAln	**0.078**	**0.056**	0.052	**0.165**
–GlaHom	**0.052**	0.038	0.011	**0.170**
–GlaMid	**0.086**	0.044	**0.107**	**0.272**
–GlaQCI	**0.080**	0.086	**0.232**	**0.219**
–GlaVan	**0.103**	0.069	**0.171**	**0.265**
–GlaWA	**0.110**	0.113	0.059	**0.274**
–GlaOR	**0.098**	0.056	0.059	**0.199**
–CanRus	**0.141**	**0.211**	**0.743**	**0.221**
–CanAKC	**0.128**	**0.217**	**0.592**	**0.312**
–CanAnc	**0.176**	**0.236**	**0.468**	**0.210**
–CanNWT	**0.148**	**0.202**	**0.744**	**0.164**
–CanSw	**0.270**	0.119	**0.879**	**0.219**
Gld				
–VegYa	**0.088**	-0.057	**0.287**	0.039
–VegCh	0.034	0.032	0.100	-0.044

–SmiAK	0.015	0.048	0.086	0.016
–SmiNWT	0.018	0.026	**0.155**	0.049
–SmiMN	0.007	-0.052	**0.225**	-0.002
–SmiMD	0.018	0.050	**0.239**	**0.123**
–SmiNY	0.048	0.014	**0.401**	0.098
–SmiNFL	**0.062**	0.066	**0.406**	0.037
–AeIc	0.047	-0.007	**0.376**	**0.079**
–AeFrc	**0.064**	0.044	**0.193**	0.002
–AaTrm	0.014	0.045	**0.536**	0.078
–HypNS	**0.040**	0.019	**0.070**	0.022
–HypYKD	0.016	-0.014	**0.130**	-0.024
–HypBfn	**0.084**	**0.109**	0.091	0.000
–HypGrn	**0.058**	**0.067**	0.171	0.009
–HypIc	**0.128**	0.021	**0.794**	**0.132**
–HypSvd	0.048	**0.063**	**0.821**	0.015
–GlaAln	**0.092**	**0.104**	**0.095**	**0.142**
–GlaHom	**0.054**	0.038	0.083	**0.144**
–GlaMid	**0.109**	**0.139**	**0.146**	**0.281**
–GlaQCI	**0.119**	**0.178**	**0.261**	**0.252**
–GlaVan	**0.156**	**0.261**	**0.208**	**0.302**
–GlaWA	**0.160**	**0.277**	0.084	**0.280**
–GlaOR	**0.142**	**0.374**	**0.175**	**0.233**
–CanRus	**0.152**	0.046	**0.753**	**0.325**

–CanAKC	**0.178**	**0.296**	**0.610**	**0.368**
–CanAnc	**0.226**	**0.339**	**0.491**	**0.269**
–CanNWT	**0.193**	**0.302**	**0.749**	**0.175**
–CanSw	**0.274**	**0.210**	**0.882**	**0.342**
VegYa				
–VegCh	0.014	0.033	0.107	-0.019
–SmiAK	0.012	-0.109	0.112	-0.103
–SmiNWT	**0.052**	0.069	-0.022	-0.013
–SmiMN	**0.080**	-0.060	0.032	0.072
–SmiMD	**0.089**	-0.016	-0.063	**0.086**
–SmiNY	0.037	-0.099	**0.087**	0.057
–SmiNFL	**0.191**	0.054	0.056	0.035
–AeIc	**0.121**	0.071	0.192	**0.231**
–AeFrc	**0.088**	0.072	-0.016	0.017
–AaTrm	**0.071**	**0.131**	**0.398**	**0.189**
–HypNS	**0.118**	0.051	**0.290**	0.039
–HypYKD	0.017	-0.101	**0.378**	0.048
–HypBfn	**0.075**	0.101	**0.283**	**0.082**
–HypGrn	**0.052**	0.057	0.129	**0.095**
–HypIc	**0.219**	0.034	**0.731**	**0.306**
–HypSvd	**0.131**	-0.060	**0.769**	0.028
–GlaAln	**0.054**	-0.108	**0.196**	0.014
–GlaHom	0.033	-0.152	**0.194**	-0.002

–GlaMid	0.047	-0.168	0.128	0.086
–GlaQCI	**0.075**	-0.163	0.089	0.030
–GlaVan	**0.105**	-0.092	**0.255**	0.085
–GlaWA	**0.084**	-0.026	0.083	0.109
–GlaOR	**0.141**	-0.051	**0.432**	0.039
–CanRus	**0.098**	-0.012	**0.700**	**0.269**
–CanAKC	**0.074**	**0.191**	**0.584**	**0.327**
–CanAnc	**0.128**	**0.243**	**0.486**	**0.203**
–CanNWT	**0.088**	**0.197**	**0.749**	**0.083**
–CanSw	**0.238**	-0.038	**0.853**	**0.208**
VegCh				
–SmiAK	-0.013	0.043	-0.098	-0.037
–SmiNWT	0.010	0.040	**0.154**	0.059
–SmiMN	-0.006	-0.039	-0.070	0.036
–SmiMD	0.016	0.062	0.072	**0.134**
–SmiNY	0.033	0.015	**0.250**	**0.148**
–SmiNFL	**0.101**	**0.178**	**0.327**	0.031
–AeIc	**0.095**	**0.121**	**0.179**	**0.120**
–AeFrc	**0.080**	0.076	**0.097**	-0.014
–AaTrm	0.038	0.067	**0.337**	**0.074**
–HypNS	**0.053**	0.089	0.053	0.010
–HypYKD	0.026	0.004	**0.148**	0.018
–HypBfn	**0.056**	**0.120**	0.035	0.025

–HypGrn	0.016	**0.189**	0.078	0.011
–HypIc	**0.204**	**0.200**	**0.608**	**0.201**
–HypSvd	**0.068**	0.004	**0.639**	0.015
–GlaAln	0.035	0.031	-0.029	**0.147**
–GlaHom	-0.015	-0.092	0.047	**0.151**
–GlaMid	0.023	-0.018	0.009	**0.300**
–GlaQCI	0.027	-0.019	0.118	**0.246**
–GlaVan	**0.098**	0.041	0.081	**0.308**
–GlaWA	**0.091**	0.065	-0.053	**0.286**
–GlaOR	**0.124**	0.107	**0.125**	**0.195**
–CanRus	**0.035**	0.111	**0.628**	**0.220**
–CanAKC	**0.061**	**0.190**	**0.405**	**0.261**
–CanAnc	**0.076**	**0.208**	**0.326**	**0.146**
–CanNWT	**0.061**	**0.171**	**0.644**	**0.096**
–CanSw	**0.117**	0.078	**0.726**	**0.175**
SmiAK				
–SmiNWT	0.005	**0.083**	0.101	-0.028
–SmiMN	-0.026	-0.048	0.050	0.100
–SmiMD	0.050	**0.082**	0.090	0.030
–SmiNY	0.046	0.000	**0.404**	0.103
–SmiNFL	**0.100**	**0.182**	**0.346**	-0.037
–AeIc	**0.078**	**0.125**	0.201	**0.281**
–AeFrc	**0.074**	**0.143**	0.100	0.024

–AaTrm	**0.053**	**0.162**	**0.403**	**0.232**
–HypNS	0.015	**0.090**	0.068	0.094
–HypYKD	0.010	-0.017	0.082	0.046
–HypBfn	**0.056**	**0.145**	0.107	**0.112**
–HypGrn	0.039	**0.114**	0.024	**0.104**
–HypIc	**0.167**	**0.100**	**0.736**	**0.357**
–HypSvd	0.061	0.044	**0.769**	0.076
–GlaAln	0.035	0.031	0.009	0.008
–GlaHom	-0.004	0.003	-0.006	0.017
–GlaMid	0.042	-0.005	0.029	0.110
–GlaQCI	0.050	0.017	0.118	0.068
–GlaVan	**0.082**	**0.105**	0.071	0.091
–GlaWA	**0.082**	**0.129**	-0.014	0.088
–GlaOR	**0.101**	**0.188**	**0.156**	0.011
–CanRus	**0.087**	**0.163**	**0.696**	**0.227**
–CanAKC	**0.123**	**0.339**	**0.508**	**0.210**
–CanAnc	**0.156**	**0.370**	**0.398**	0.086
–CanNWT	**0.132**	**0.313**	**0.715**	-0.008
–CanSw	**0.201**	**0.138**	**0.853**	-0.027
SmiNWT				
–SmiMN	-0.013	0.075	0.081	0.054
–SmiMD	0.018	**0.045**	0.060	0.041
–SmiNY	0.031	0.019	-0.031	-0.004

–SmiNFL	**0.050**	**0.121**	0.012	0.032
–AeIc	**0.047**	0.002	**0.304**	**0.203**
–AeFrc	**0.049**	0.007	0.021	0.036
–AaTrm	0.026	-0.010	**0.485**	**0.191**
–HypNS	0.004	-0.014	**0.248**	**0.078**
–HypYKD	**0.032**	0.028	**0.283**	0.025
–HypBfn	0.011	0.032	**0.236**	**0.075**
–HypGrn	0.013	**0.042**	**0.150**	**0.102**
–HypIc	**0.093**	**0.060**	**0.727**	**0.247**
–HypSvd	0.010	**0.042**	**0.757**	0.045
–GlaAln	**0.097**	**0.176**	**0.204**	0.002
–GlaHom	**0.064**	**0.072**	**0.179**	-0.018
–GlaMid	**0.108**	**0.194**	**0.195**	0.057
–GlaQCI	**0.114**	**0.229**	**0.175**	**0.058**
–GlaVan	**0.159**	**0.316**	**0.282**	**0.061**
–GlaWA	**0.152**	**0.319**	**0.127**	**0.070**
–GlaOR	**0.162**	**0.417**	**0.328**	0.058
–CanRus	**0.128**	**0.107**	**0.757**	**0.357**
–CanAKC	**0.169**	**0.393**	**0.668**	**0.359**
–CanAnc	**0.198**	**0.427**	**0.556**	**0.261**
–CanNWT	**0.175**	**0.374**	**0.761**	**0.123**
–CanSw	**0.239**	**0.247**	**0.852**	**0.286**
SmiMN				

–SmiMD	0.010	-0.009	-0.085	**0.071**
–SmiNY	0.048	-0.077	0.129	0.025
–SmiNFL	**0.071**	0.046	0.183	0.046
–AeIc	**0.114**	0.060	0.114	0.014
–AeFrc	**0.091**	0.055	-0.031	-0.008
–AaTrm	0.061	**0.109**	**0.275**	0.036
–HypNS	0.054	0.069	**0.180**	0.026
–HypYKD	0.021	-0.094	**0.270**	-0.040
–HypBfn	**0.076**	**0.107**	0.151	-0.047
–HypGrn	0.044	0.096	0.085	-0.013
–HypIc	**0.192**	0.077	**0.600**	**0.031**
–HypSvd	**0.068**	-0.117	**0.641**	-0.005
–GlaAln	0.042	-0.106	0.036	**0.116**
–GlaHom	0.002	-0.195	0.107	0.135
–GlaMid	0.043	-0.150	0.021	**0.323**
–GlaQCI	0.033	-0.171	0.044	**0.305**
–GlaVan	**0.104**	-0.088	0.107	**0.370**
–GlaWA	**0.110**	-0.015	-0.053	**0.304**
–GlaOR	**0.132**	-0.051	**0.263**	**0.291**
–CanRus	0.054	-0.045	**0.656**	**0.447**
–CanAKC	**0.081**	**0.204**	**0.437**	**0.490**
–CanAnc	**0.126**	**0.240**	**0.370**	**0.373**
–CanNWT	**0.092**	**0.188**	**0.680**	**0.251**

–CanSw	**0.202**	-0.085	**0.769**	**0.426**
SmiMD				
–SmiNY	-0.014	-0.026	0.058	-0.056
–SmiNFL	-0.002	-0.016	0.083	-0.005
–AeIc	**0.087**	0.020	**0.178**	**0.246**
–AeFrc	**0.095**	0.069	0.010	**0.080**
–AaTrm	0.036	**0.089**	**0.318**	**0.242**
–HypNS	**0.076**	0.007	**0.251**	**0.152**
–HypYKD	**0.076**	0.047	**0.312**	0.051
–HypBfn	**0.042**	-0.035	**0.222**	**0.102**
–HypGrn	0.049	-0.017	0.127	**0.123**
–HypIc	**0.147**	-0.002	**0.600**	**0.275**
–HypSvd	**0.043**	0.028	**0.636**	**0.106**
–GlaAln	**0.124**	**0.133**	**0.156**	0.029
–GlaHom	**0.064**	0.037	**0.151**	0.029
–GlaMid	**0.115**	**0.154**	**0.107**	**0.132**
–GlaQCI	**0.134**	**0.176**	0.094	**0.153**
–GlaVan	**0.213**	**0.270**	**0.190**	**0.150**
–GlaWA	**0.215**	**0.307**	0.029	**0.109**
–GlaOR	**0.220**	**0.389**	**0.282**	**0.141**
–CanRus	**0.164**	0.040	**0.656**	**0.454**
–CanAKC	**0.180**	**0.369**	**0.502**	**0.455**
–CanAnc	**0.220**	**0.364**	**0.434**	**0.363**

–CanNWT	**0.184**	**0.356**	**0.698**	**0.211**
–CanSw	**0.246**	**0.137**	**0.747**	**0.382**
SmiNY				
–SmiNFL	**0.065**	0.034	-0.051	0.006
–AeIc	**0.086**	0.018	**0.300**	**0.217**
–AeFrc	**0.069**	0.030	0.023	0.068
–AaTrm	0.034	0.058	**0.494**	**0.230**
–HypNS	**0.068**	-0.015	**0.352**	**0.148**
–HypYKD	**0.066**	0.014	**0.489**	0.010
–HypBfn	**0.040**	0.015	**0.383**	**0.075**
–HypGrn	0.024	-0.006	**0.172**	**0.105**
–HypIc	**0.156**	-0.004	**0.826**	**0.236**
–HypSvd	**0.048**	0.020	**0.863**	0.093
–GlaAln	**0.140**	**0.115**	**0.255**	-0.018
–GlaHom	**0.086**	0.034	**0.306**	0.013
–GlaMid	**0.128**	**0.117**	**0.210**	**0.143**
–GlaQCI	**0.162**	**0.144**	**0.213**	**0.188**
–GlaVan	**0.220**	**0.246**	**0.385**	**0.185**
–GlaWA	**0.211**	**0.272**	**0.169**	**0.117**
–GlaOR	**0.234**	**0.348**	**0.655**	**0.167**
–CanRus	**0.163**	0.069	**0.784**	**0.504**
–CanAKC	**0.192**	**0.342**	**0.664**	**0.497**
–CanAnc	**0.230**	**0.363**	**0.554**	**0.394**

–CanNWT	**0.186**	**0.341**	**0.786**	**0.224**
–CanSw	**0.256**	0.112	**0.947**	**0.394**
SmiNFL				
–AeIc	**0.134**	0.038	**0.351**	**0.172**
–AeFrc	**0.119**	**0.109**	**0.069**	0.037
–AaTrm	**0.085**	**0.145**	**0.536**	**0.163**
–HypNS	**0.103**	**0.069**	**0.400**	**0.081**
–HypYKD	**0.135**	**0.100**	**0.495**	0.022
–HypBfn	**0.089**	**0.060**	**0.432**	**0.054**
–HypGrn	**0.107**	0.050	**0.207**	**0.068**
–HypIc	**0.152**	0.025	**0.809**	**0.208**
–HypSvd	**0.052**	**0.098**	**0.840**	**0.055**
–GlaAln	**0.179**	**0.204**	**0.306**	**0.055**
–GlaHom	**0.123**	**0.116**	**0.349**	0.048
–GlaMid	**0.170**	**0.262**	**0.277**	**0.132**
–GlaQCI	**0.183**	**0.296**	**0.241**	**0.126**
–GlaVan	**0.267**	**0.396**	**0.422**	**0.126**
–GlaWA	**0.275**	**0.431**	**0.230**	**0.127**
–GlaOR	**0.271**	**0.533**	**0.597**	**0.111**
–CanRus	**0.236**	0.013	**0.813**	**0.331**
–CanAKC	**0.276**	**0.442**	**0.728**	**0.340**
–CanAnc	**0.317**	**0.450**	**0.622**	**0.259**
–CanNWT	**0.268**	**0.411**	**0.806**	**0.143**

–CanSw	**0.335**	**0.242**	**0.925**	**0.308**
AeIc				
–AeFrc	0.005	-0.008	**0.136**	**0.057**
–AaTrm	0.029	0.012	0.036	-0.021
–HypNS	**0.077**	-0.022	**0.377**	0.053
–HypYKD	**0.043**	0.032	**0.409**	**0.057**
–HypBfn	**0.065**	**0.046**	**0.380**	-0.008
–HypGrn	0.022	0.025	0.106	0.004
–HypIc	0.040	0.033	**0.189**	-0.024
–HypSvd	0.038	0.054	**0.240**	0.046
–GlaAln	**0.150**	**0.198**	**0.283**	**0.288**
–GlaHom	**0.140**	**0.088**	**0.323**	**0.320**
–GlaMid	**0.187**	**0.231**	0.092	**0.480**
–GlaQCI	**0.174**	**0.272**	0.076	**0.459**
–GlaVan	**0.234**	**0.351**	**0.214**	**0.521**
–GlaWA	**0.233**	**0.365**	**0.210**	**0.470**
–GlaOR	**0.230**	**0.459**	**0.399**	**0.460**
–CanRus	**0.217**	0.027	**0.552**	**0.498**
–CanAKC	**0.247**	**0.384**	**0.465**	**0.548**
–CanAnc	**0.284**	**0.405**	**0.389**	**0.456**
–CanNWT	**0.236**	**0.367**	**0.625**	**0.346**
–CanSw	**0.357**	**0.260**	**0.615**	**0.533**
AeFrc				

–AaTrm	0.013	-0.027	**0.306**	0.020
–HypNS	**0.091**	0.002	**0.249**	-0.027
–HypYKD	**0.064**	0.065	**0.290**	0.000
–HypBfn	**0.084**	0.066	**0.235**	-0.019
–HypGrn	**0.038**	**0.084**	0.089	-0.008
–HypIc	**0.086**	0.091	**0.595**	**0.117**
–HypSvd	0.031	**0.067**	**0.629**	-0.041
–GlaAln	**0.181**	**0.225**	**0.181**	**0.108**
–GlaHom	**0.153**	**0.104**	**0.175**	**0.093**
–GlaMid	**0.196**	**0.237**	0.077	**0.213**
–GlaQCI	**0.195**	**0.271**	0.037	**0.185**
–GlaVan	**0.254**	**0.348**	**0.204**	**0.230**
–GlaWA	**0.241**	**0.356**	0.092	**0.215**
–GlaOR	**0.255**	**0.442**	**0.308**	**0.179**
–CanRus	**0.180**	0.053	**0.677**	**0.305**
–CanAKC	**0.239**	**0.368**	**0.563**	**0.336**
–CanAnc	**0.266**	**0.407**	**0.457**	**0.235**
–CanNWT	**0.220**	**0.360**	**0.704**	**0.133**
–CanSw	**0.322**	**0.212**	**0.772**	**0.301**
AaTrm				
–HypNS	**0.050**	0.009	**0.520**	0.009
–HypYKD	**0.060**	**0.068**	**0.569**	**0.074**
–HypBfn	**0.065**	**0.074**	**0.532**	-0.002

–HypGrn	**0.040**	**0.106**	**0.244**	-0.005
–HypIc	**0.120**	**0.117**	0.091	0.038
–HypSvd	0.037	**0.071**	0.155	0.012
–GlaAln	**0.136**	**0.236**	**0.417**	**0.281**
–GlaHom	**0.101**	**0.117**	**0.485**	**0.296**
–GlaMid	**0.143**	**0.247**	**0.219**	**0.453**
–GlaQCI	**0.166**	**0.279**	**0.259**	**0.419**
–GlaVan	**0.209**	**0.356**	**0.361**	**0.494**
–GlaWA	**0.194**	**0.357**	**0.351**	**0.444**
–GlaOR	**0.191**	**0.447**	**0.564**	**0.419**
–CanRus	**0.154**	**0.083**	**0.579**	**0.428**
–CanAKC	**0.201**	**0.351**	**0.482**	**0.489**
–CanAnc	**0.242**	**0.387**	**0.436**	**0.388**
–CanNWT	**0.201**	**0.345**	**0.642**	**0.291**
–CanSw	**0.265**	**0.244**	**0.657**	**0.472**
HypNS				
–HypYKD	**0.043**	0.024	0.022	0.034
–HypBfn	0.025	0.028	-0.037	-0.005
–HypGrn	0.030	0.052	**0.201**	0.002
–HypIc	**0.161**	0.044	**0.709**	**0.125**
–HypSvd	0.030	0.040	**0.732**	-0.032
–GlaAln	**0.125**	**0.178**	0.012	**0.166**
–GlaHom	**0.080**	0.060	0.020	**0.156**

–GlaMid	**0.139**	**0.205**	**0.133**	**0.275**
–GlaQCI	**0.152**	**0.245**	**0.255**	**0.240**
–GlaVan	**0.187**	**0.343**	**0.120**	**0.293**
–GlaWA	**0.185**	**0.359**	0.064	**0.279**
–GlaOR	**0.200**	**0.465**	0.001	**0.238**
–CanRus	**0.155**	**0.071**	**0.729**	**0.310**
–CanAKC	**0.224**	**0.434**	**0.564**	**0.349**
–CanAnc	**0.254**	**0.459**	**0.447**	**0.247**
–CanNWT	**0.213**	**0.398**	**0.714**	**0.157**
–CanSw	**0.278**	**0.252**	**0.810**	**0.314**
HypYKD				
–HypBfn	**0.056**	**0.081**	**0.094**	-0.023
–HypGrn	**0.032**	**0.040**	**0.231**	0.006
–HypIc	**0.126**	0.024	**0.792**	**0.082**
–HypSvd	**0.075**	0.000	**0.816**	0.006
–GlaAln	**0.052**	**0.078**	0.047	**0.088**
–GlaHom	**0.036**	0.057	-0.013	0.095
–GlaMid	**0.083**	**0.091**	**0.173**	**0.230**
–GlaQCI	**0.077**	**0.117**	**0.304**	**0.226**
–GlaVan	**0.105**	**0.204**	**0.154**	**0.252**
–GlaWA	**0.109**	**0.211**	**0.100**	**0.227**
–GlaOR	**0.109**	**0.277**	-0.038	**0.213**
–CanRus	**0.153**	**0.074**	**0.761**	**0.395**

–CanAKC	**0.156**	**0.258**	**0.608**	**0.412**
–CanAnc	**0.195**	**0.306**	**0.481**	**0.322**
–CanNWT	**0.171**	**0.270**	**0.748**	**0.204**
–CanSw	**0.268**	**0.131**	**0.876**	**0.381**
HypBfn				
–HypGrn	0.011	0.018	**0.235**	-0.028
–HypIc	**0.087**	0.060	**0.752**	0.029
–HypSvd	0.016	0.028	**0.777**	-0.024
–GlaAln	**0.145**	**0.213**	0.035	**0.149**
–GlaHom	**0.111**	**0.108**	0.054	**0.161**
–GlaMid	**0.167**	**0.228**	**0.146**	**0.317**
–GlaQCI	**0.170**	**0.253**	**0.250**	**0.298**
–GlaVan	**0.230**	**0.343**	**0.164**	**0.354**
–GlaWA	**0.231**	**0.365**	0.068	**0.311**
–GlaOR	**0.249**	**0.454**	0.097	**0.292**
–CanRus	**0.199**	0.082	**0.735**	**0.409**
–CanAKC	**0.237**	**0.422**	**0.558**	**0.446**
–CanAnc	**0.271**	**0.416**	**0.447**	**0.346**
–CanNWT	**0.232**	**0.388**	**0.727**	**0.230**
–CanSw	**0.307**	**0.199**	**0.837**	**0.417**
HypGrn				
–HypIc	**0.011**	0.018	**0.472**	**0.045**
–HypSvd	0.028	**0.052**	**0.509**	-0.008

–GlaAln	**0.124**	**0.206**	**0.161**	**0.171**
–GlaHom	**0.092**	**0.124**	**0.160**	**0.179**
–GlaMid	**0.139**	**0.236**	0.024	**0.305**
–GlaQCI	**0.138**	**0.275**	0.085	**0.287**
–GlaVan	**0.207**	**0.380**	**0.153**	**0.321**
–GlaWA	**0.204**	**0.401**	**0.118**	**0.302**
–GlaOR	**0.225**	**0.503**	**0.243**	**0.276**
–CanRus	**0.140**	0.040	**0.644**	**0.357**
–CanAKC	**0.193**	**0.440**	**0.512**	**0.391**
–CanAnc	**0.211**	**0.449**	**0.387**	**0.305**
–CanNWT	**0.186**	**0.403**	**0.649**	**0.216**
–CanSw	**0.236**	**0.229**	**0.721**	**0.380**
HypIc				
–HypSvd	**0.076**	0.044	0.042	**0.112**
–GlaAln	**0.227**	**0.177**	**0.595**	**0.322**
–GlaHom	**0.241**	**0.113**	**0.726**	**0.372**
–GlaMid	**0.285**	**0.213**	**0.422**	**0.543**
–GlaQCI	**0.266**	**0.253**	**0.516**	**0.528**
–GlaVan	**0.342**	**0.355**	**0.603**	**0.593**
–GlaWA	**0.344**	**0.378**	**0.567**	**0.526**
–GlaOR	**0.354**	**0.483**	**0.818**	**0.532**
–CanRus	**0.329**	0.050	**0.687**	**0.575**
–CanAKC	**0.357**	**0.412**	**0.603**	**0.622**

–CanAnc	**0.395**	**0.429**	**0.558**	**0.533**
–CanNWT	**0.335**	**0.377**	**0.731**	**0.412**
–CanSw	**0.488**	**0.249**	**0.828**	**0.600**
HypSvd				
–GlaAln	**0.191**	**0.163**	**0.618**	**0.124**
–GlaHom	**0.150**	**0.119**	**0.751**	**0.115**
–GlaMid	**0.209**	**0.164**	**0.438**	**0.249**
–GlaQCI	**0.207**	**0.175**	**0.541**	**0.219**
–GlaVan	**0.273**	**0.278**	**0.636**	**0.277**
–GlaWA	**0.267**	**0.288**	**0.593**	**0.249**
–GlaOR	**0.278**	**0.346**	**0.844**	**0.217**
–CanRus	**0.184**	0.072	**0.685**	**0.344**
–CanAKC	**0.259**	**0.289**	**0.603**	**0.376**
–CanAnc	**0.290**	**0.310**	**0.554**	**0.268**
–CanNWT	**0.245**	**0.284**	**0.728**	**0.155**
–CanSw	**0.307**	0.062	**0.838**	**0.329**
GlaAln				
–GlaHom	-0.017	-0.003	0.007	-0.016
–GlaMid	-0.003	-0.017	**0.075**	0.050
–GlaQCI	0.001	-0.002	**0.178**	0.075
–GlaVan	0.021	0.060	0.031	0.054
–GlaWA	0.032	**0.111**	-0.028	0.051
–GlaOR	0.030	**0.221**	0.008	0.071

–CanRus	**0.190**	**0.225**	**0.709**	**0.443**
–CanAKC	**0.161**	**0.350**	**0.533**	**0.432**
–CanAnc	**0.202**	**0.367**	**0.420**	**0.337**
–CanNWT	**0.177**	**0.322**	**0.715**	**0.181**
–CanSw	**0.282**	**0.223**	**0.816**	**0.309**
GlaHom				
–GlaMid	-0.025	0.021	**0.105**	-0.017
–GlaQCI	-0.016	0.045	**0.189**	0.006
–GlaVan	0.016	**0.110**	0.113	-0.016
–GlaWA	0.034	**0.150**	0.002	-0.011
–GlaOR	0.034	**0.253**	-0.015	0.001
–CanRus	**0.140**	**0.167**	**0.520**	**0.426**
–CanAKC	**0.125**	**0.338**	**0.294**	**0.411**
–CanAnc	**0.160**	**0.343**	**0.178**	**0.297**
–CanNWT	**0.143**	**0.330**	**0.508**	**0.127**
–CanSw	**0.218**	**0.178**	**0.588**	**0.277**
GlaMid				
–GlaQCI	-0.024	-0.049	0.025	-0.025
–GlaVan	-0.002	-0.009	0.084	-0.050
–GlaWA	0.014	0.024	0.054	-0.039
–GlaOR	0.023	0.090	**0.151**	-0.028
–CanRus	**0.178**	**0.269**	**0.624**	**0.499**
–CanAKC	**0.123**	**0.315**	**0.493**	**0.478**

–CanAnc	**0.158**	**0.328**	**0.388**	**0.352**
–CanNWT	**0.139**	**0.295**	**0.668**	**0.151**
–CanSw	**0.248**	**0.161**	**0.712**	**0.299**
GlaQCI				
–GlaVan	0.002	-0.015	0.133	-0.047
–GlaWA	0.039	0.021	**0.113**	-0.010
–GlaOR	0.043	0.076	**0.319**	-0.056
–CanRus	**0.198**	**0.296**	**0.665**	**0.419**
–CanAKC	**0.142**	**0.311**	**0.485**	**0.391**
–CanAnc	**0.162**	**0.311**	**0.404**	**0.261**
–CanNWT	**0.150**	**0.281**	**0.692**	**0.091**
–CanSw	**0.269**	0.146	**0.754**	**0.174**
GlaVan				
–GlaWA	-0.026	-0.037	0.041	-0.050
–GlaOR	-0.024	0.006	0.136	-0.068
–CanRus	**0.237**	**0.379**	**0.623**	**0.495**
–CanAKC	**0.166**	**0.338**	**0.426**	**0.486**
–CanAnc	**0.202**	**0.328**	**0.353**	**0.341**
–CanNWT	**0.175**	**0.303**	**0.642**	**0.128**
–CanSw	**0.342**	**0.240**	**0.687**	**0.268**
GlaWA				
–GlaOR	-0.022	-0.032	0.038	-0.028
–CanRus	**0.214**	**0.399**	**0.751**	**0.492**

–CanAKC	**0.159**	**0.326**	**0.563**	**0.471**
–CanAnc	**0.188**	**0.328**	**0.449**	**0.354**
–CanNWT	**0.168**	**0.284**	**0.748**	**0.164**
–CanSw	**0.323**	**0.269**	**0.898**	**0.315**
GlaOR				
–CanRus	**0.268**	**0.468**	**0.656**	**0.395**
–CanAKC	**0.193**	**0.325**	**0.461**	**0.380**
–CanAnc	**0.245**	**0.311**	**0.379**	**0.245**
–CanNWT	**0.201**	**0.270**	**0.648**	**0.082**
–CanSw	**0.406**	**0.252**	**0.718**	**0.189**
CanRus				
–CanAKC	**0.096**	**0.272**	**0.478**	0.046
–CanAnc	**0.094**	**0.303**	**0.452**	0.018
–CanNWT	**0.103**	**0.313**	**0.559**	**0.142**
–CanSw	0.020	0.139	0.028	-0.061
CanAKC				
–CanAnc	0.003	-0.013	0.053	0.007
–CanNWT	-0.013	-0.011	**0.188**	**0.090**
–CanSw	**0.161**	**0.205**	**0.561**	0.019
CanAnc				
–CanNWT	0.000	-0.012	**0.155**	0.025
–CanSw	**0.135**	**0.210**	**0.544**	-0.014
CanNWT				

–CanSw	**0.139**	**0.224**	**0.677**	0.035